


RESEARCH REPORT

Distress-dependent temporal variability of regions encoding domain-specific and domain-general behavioral manifestations of phantom percepts

Anusha Mohan¹  | Dirk De Ridder² | Rajith Idiculla¹ | Clisha DSouza¹ | Sven Vanneste¹

¹Lab for Clinical & Integrative Neuroscience, School of Behavioral and Brain Sciences, The University of Texas at Dallas, Richardson, Texas

²Department of Surgical Sciences, Section of Neurosurgery, Dunedin School of Medicine, University of Otago, Dunedin, New Zealand

Correspondence

Sven Vanneste, Lab for Clinical & Integrative Neuroscience, School of Behavioral & Brain Science, University of Texas at Dallas, Richardson, TX.
Email: sven.vanneste@utdallas.edu

Abstract

Tinnitus is the perception of a phantom sound characterized behaviorally by a loudness and a distress component. Although a wealth of information is available about the relationship between these behavioral correlates and changes in static functional connectivity, its relationship with dynamic changes in network connectivity is yet unexplored. The aim of this study was thus to investigate changes in the flexibility and stability of temporal variability in tinnitus and its relation to loudness and distress using continuous resting-state EEG. We observe an increase in temporal variability at the whole-brain level in tinnitus, which is spatiotemporally distributed at the nodal level. Behaviorally, we observe changes in the relationship between temporal variability and loudness and distress depending on the amount of distress experienced. In patients with low distress, there is no relationship between temporal variability and loudness or distress, demonstrating a resilience in dynamic connectivity of the brain. However, patients with high distress exhibit a direct relationship with increasing loudness in the primary auditory cortex and parahippocampus, and an inverse relationship with increasing distress in the parahippocampus. In tinnitus, the specific sensory (loudness) component related to increased temporal variability possibly reflects a Bayesian search for updating deafferentation-based missing information. On the other hand, the decreased temporal variability related to the nonspecific distress component possibly reflects a more hard-wired or less adaptive contextual processing. Therefore, our findings may reveal a way to understand the changes in network dynamics not just in tinnitus, but also in other brain disorders.

KEYWORDS

dynamic connectivity, EEG, sLORETA, tinnitus

Abbreviations: A1, primary auditory cortex; ADHD, attention-deficit/hyperactivity disorder; ANOVA, analysis of variance; BOLD, blood oxygen level dependent; dACC, dorsal anterior cingulate cortex; ECG, electrocardiography; EEG, electroencephalography; MEG, magnetoencephalography; PHC, parahippocampus; rsfMRI, resting-state functional magnetic resonance imaging; sgACC, subgenual anterior cingulate cortex; sLORETA, standardized low-resolution brain electromagnetic tomography; TQ, Tinnitus Questionnaire; VAS, visual analog scale.

Edited by Christoph M. Michel. Reviewed by Muthuramam Muthuramam, Johannes Gutenberg University Mainz, Germany; and Dimitri van de Ville, EPFL and UniGE, Switzerland

All peer review communications can be found with the online version of the article.

1 | INTRODUCTION

“Communication through coherence” or simply, functional connectivity between brain regions, is extensively studied using resting-state fMRI (rsfMRI), electroencephalography (EEG) and magnetoencephalography (MEG). These neuroimaging techniques use temporal changes in neural activity (or blood-oxygen-level-dependent (BOLD) signal) at different sources across the entire stretch of recording to compute the phase coherence (or correlation) between different brain regions (van den Heuvel & Sporns, 2013; Stam, 2014). This measure describes the architecture and topology of a network as if the network is static, that is, by assuming that the coherence does not change across the duration of the recording (Hindriks et al., 2016).

Although static functional networks describe key features of information sharing between brain regions, they fail to capture the dynamic strengthening or weakening of connections that are critical to maintain a balance between excitation and inhibition (Arnsten, Paspalas, Gamo, Yang, & Wang, 2010). The temporal changes in functional connectivity in both stimulus-evoked and resting brain activity are accompanied by subsequent spatial variations, which enable active switching of connectivity within and between communities of brain regions (Deco & Kringelbach, 2016). This permits a dynamic interaction between modular, highly specialized stimulus processing (segregation) and more global interaction amongst different modules (integration). Therefore, the integration of modular brain networks is not static but dynamic over the length of the recording, providing multiple routes for information transfer (Deco & Kringelbach, 2016).

Dynamic functional connectivity has been explored using different functional modalities in both healthy and clinical populations. Previous research using fMRI showed that temporal changes in functional connectivity in healthy adults were associated with flexibility and the ability to adapt to changes in the environment (Zhang et al., 2016). This property was also associated with the dynamic reconfiguration of the brain in learning and memory (Bassett et al., 2011). On the other hand, pathological variations in dynamic functional connectivity were associated with corresponding changes in behavioral symptoms of that particular disorder. Barttfeld et al. (2014) observed a decrease in temporal variability of functional connectivity using EEG in patients with bipolar disorder. On the contrary, they observed an increase in temporal variability in patients with attention-deficit/hyperactivity disorder (ADHD; Barttfeld et al., 2014). These findings agree with the results obtained by Zhang et al. using fMRI. These changes were shown specifically in regions of the default mode network (Zhang et al., 2016). Further, Zhang et al. (2016) also showed a decrease in temporal variability of the default mode regions and the medial temporal regions

in schizophrenia associated with rumination over one's thoughts. This agrees with the results of Kaiser et al. (2015) who showed a decrease in temporal variability of functional connectivity (using fMRI) specifically at the parahippocampus as a correlate of rumination in patients with major depressive disorder (MDD). Thus, temporal variability of functional connectivity is an important biomarker that captures the dynamic nature of physiological variables. Therefore, this study investigates the pathological changes in temporal variability of functional connectivity calculated from resting-state EEG in patients with chronic tinnitus compared to healthy adults. This study also relates these changes to different behavioral symptoms of the disorder.

Tinnitus is the continuous perception of a phantom sound in the absence of an external auditory stimulus (Jastreboff, 1990). The incidence of tinnitus is strongly associated with different types of hearing loss (Jansen, Helleman, Dreschler, & de Laat, 2009; Plack, Barker, & Prendergast, 2014; Plack, Prendergast, & Hall, 2015; Szymiec, Dabrowski, Banaszewski, & Szyfter, 2002). Sensory deafferentation with or without hearing loss (Langers, de Kleine, & van Dijk, 2012; Vanneste & De Ridder, 2016) is proposed to create a prediction error between the bottom-up sensory input and the top-down predictions of the brain regarding incoming stimuli (De Ridder, Vanneste, & Freeman, 2014). Therefore, tinnitus is hypothesized to be a maladaptive percept generated by the brain to compensate for this prediction error (Mohan & Vanneste, 2017).

Behaviorally, tinnitus is characterized by a specific sensory component (loudness) and a nonspecific emotional component (distress). The loudness of the tinnitus percept was shown to be encoded by an increase in gamma activity in the auditory cortex and modulated by connections between auditory regions and medial temporal regions such as the parahippocampus (De Ridder & Vanneste, 2014; Vanneste & De Ridder, 2016). The loudness of the tinnitus percept is also directly related to the amount of deafferentation encoded by the theta frequency band (De Ridder, Vanneste, & Freeman, 2014; De Ridder, Vanneste, Weisz, et al., 2014). Furthermore, the loudness of the percept is shown to be encoded by the nesting of the gamma band on the theta frequency band (De Ridder, Vanneste, Weisz, et al., 2014). The emotional component, or tinnitus-associated distress, is characterized by increased attentional focus on the percept, decreased attention to daily activity and adverse changes in stress levels, sleep quality, mood, etc. (Belli et al., 2007). This component is shown to be encoded and modulated by a network consisting of mainly the dorsal and subgenual anterior cingulate cortex, parahippocampus and other structures of the medial temporal lobe, mainly in the alpha frequency bands (De Ridder, Vanneste, Weisz, et al., 2014; Vanneste & De Ridder, 2015). This distress network is shown to be activated in not just tinnitus but other chronic neuropathologies such as chronic neuropathic

pain, fibromyalgia, post-traumatic stress disorder and dyspnea, reflecting the network's domain-general role in encoding the affective or emotional component of pathology (De Ridder, Elgoyhen, Romo, & Langguth, 2011; González-Roldán, Cifre, Sitges, & Montoya, 2016; Imperatori et al., 2014; von Leupoldt et al., 2009). Although loudness and distress are seemingly encoded by independent networks, these are proposed to be connected in highly distressed patients via the subgenual anterior cingulate cortex and the parahippocampus in the alpha frequency band, and are instrumental in associating phantom sound with distress (Vanneste, Congedo, & De Ridder, 2014).

In this study, we examine changes in the temporal dynamics of functional connectivity between the 84 Brodmann areas in tinnitus patients compared to healthy controls in different oscillatory bands and investigate how changes in temporal variability reflect upon the domain-specific loudness component and domain-general emotional/distress component of tinnitus. We further aim to analyze the dynamic interaction between the loudness and distress networks by examining the relationship between temporal variability of specific brain regions and the loudness and distress components in low- and high-distress tinnitus patients.

We evaluate temporal variability by calculating the epoch-to-epoch correlation of functional connectivity of a brain region across the time series of resting brain activity (Zhang et al., 2016). Although it was originally applied to fMRI data, we chose this method as the metric describes the whole-brain topography of temporal variability. The authors also establish a relationship between the regional functional architecture, the underlying neural activity and structural connectivity. Further, they also explain how this measure of temporal variability may be used to reflect dynamic changes in inter- and intramodular connectivity, which agree with the properties of dynamic functional connectivity as described by Deco, Tononi, Boly, and Kringelbach (2015).

Thus, applying this measure to our data, we hypothesize significant changes in temporal variability of the different Brodmann areas in the different frequency bands in the tinnitus group indicating pathological increase or decrease in temporal variability. Further, we hypothesize that these changes relate to significant changes in tinnitus symptoms such as the loudness and distress components. This study is the first of its kind, to our knowledge, to probe the temporal dynamics of maladaptive pathological compensation to sensory deprivation. In addition, it also targets to investigate changes in temporal variability of unimodal and multimodal regions encoding domain-specific and domain-general behavioral manifestations of a disorder. Thus, temporal variability discussed in this study may be a biomarker of dynamic reconfiguration of the brain in the presence of a pathology. More important, distress being a domain-general disorder, this study may be able to propose a biomarker for chronic distress. This

knowledge is a powerful tool to unravel the neurophysiology of tinnitus and potentially other neuropathologies.

2 | MATERIALS AND METHODS

2.1 | Patients with an auditory phantom percept

The patient sample consisted of 151 patients ($M = 45.87$ years; $SD = 13.25$; 102 males and 43 females) experiencing continuous and chronic (present for a year or more) tinnitus. If patients were diagnosed with any one of following disorders—pulsatile tinnitus, Ménière disease, otosclerosis, chronic headache, neurological disorders such as brain tumors or mental disorders—the person was excluded from the study. The perceived location of patients' tinnitus [left ear ($N = 43$), right ear ($N = 37$), both ears ($N = 47$)], as well the type of tinnitus [pure tone-like tinnitus ($N = 60$) or noise-like tinnitus ($N = 84$)], was noted. All patients underwent audiological testing including pure tone audiograms as well as tinnitus pitch and loudness matching. Pure tone audiometry was used to assess hearing thresholds at 0.125, 0.25, 0.5, 1, 2, 3, 4, 6 and 8 kHz ($M = 23.28$ dB HL, $SD = 16.65$) in accordance with the procedures prescribed by the British Society of Audiology (Audiology, 2008). Therefore, the pitch and loudness of the tinnitus were determined by performing an analysis of the ear contralateral to the tinnitus ear in patients with unilateral tinnitus and of the ear contralateral to the worse tinnitus ear in patients with bilateral tinnitus. A 1-kHz pure tone was presented to the ear contralateral to the (worse) tinnitus ear at an intensity that was 10 dB above the patient's hearing threshold in that ear. The pitch of the perceived tinnitus was measured by adjusting the frequency of the tone to match the pitch of the perceived tinnitus. The perceived loudness was matched to the intensity of the tone in a similar way. The tinnitus loudness in dB SL was computed as a difference between the absolute tinnitus loudness in dB HL and the audiometric threshold at the tinnitus frequency (Meeus, De Ridder, & Van de Heyning, 2011; Meeus, Heyndrickx, Lambrechts, De Ridder, & Van de Heyning, 2009).

In addition to the audiological tests, patients answered a set of questionnaires subjectively rating and describing some of the behavioral symptoms of tinnitus. A visual analog scale (VAS) for loudness ("How loud is your tinnitus?" 0 = no tinnitus and 10 = as loud as imaginable) was assessed ($M = 5.50$, $SD = 2.45$) to subjectively measure the intensity of the perceived tinnitus at that moment (Adamchic, Langguth, Hauptmann, & Tass, 2012). The Tinnitus Questionnaire (TQ) measures a broad spectrum of tinnitus-related psychological complaints (Meeus, Blaivie, & Van de Heyning, 2007). The global TQ score may be used to measure the general level of psychological and psychosomatic distress associated with the perception of a constant ringing in the ears ($M = 38.55$,

$SD = 17.24$). This study was approved by the local ethical committee (Antwerp University Hospital) and was in accordance with the declaration of Helsinki. Collection of the data was under the approval of IRB UZA OGA85. All patients gave informed consent.

2.2 | Healthy control group

A healthy control group ($N = 125$; $M = 44.04$ years; $SD = 15.33$; 45 males and 80 females) was included in the study. None of these subjects were known to suffer from tinnitus of any kind. Subjects suffering from psychiatric or neurological illness, having a history of psychiatric or drug/alcohol abuse, history of head injury (with loss of consciousness) or seizures, headache, or physical disability were excluded from the study. No hearing assessments were performed on the healthy controls.

2.3 | Data collection

Continuous resting-state EEG data were obtained from both the tinnitus and control groups (sampling rate = 500 Hz, band-passed 0.15–200 Hz) for 5 minutes during which participants were instructed to keep their eyes closed but remain awake. Participants were seated upright on a cushioned chair in a fully-lit room. EEG data were collected using 19 electrodes (Fp1, Fp2, F7, F3, Fz, F4, F8, T7, C3, Cz, C4, T8, P7, P3, Pz, P4, P8, O1, O2) placed on the scalp according to the standard 10–20 International placement, sampled using Mitsar-201 amplifiers (NovaTech <http://www.novatecheeg.com/>) and referenced to linked ears. Impedance on each of the electrodes was maintained below 5 k Ω . The data were re-sampled to 128 Hz and band-pass filtered in the range 2–44 Hz as a part of the off-line analysis. The data were then transposed into software Eureka! (Congedo, 2002), where an independent component analysis (ICA) was performed on the continuous data and was manually inspected for artifacts.

A careful inspection of artifacts was performed and all episodic artifacts suggestive of eye blinks, eye movements, jaw tension, teeth clenching, or body movement were manually removed from the EEG stream. An artifact was defined as an EEG characteristic that differs from signals generated by activity in the brain. (a) Some artifacts are known to be in a limited frequency range, for example, above some frequency. These were removed by frequency filtering. (b) Some artifacts consist of discrete frequencies such as 50 Hz (or 60 Hz for USA) or its harmonics. These were removed by notch filtering. (c) Some artifacts are limited to a certain time range, for example, in the case of eye blinks. These artifacts were recognized by visual inspection and these time intervals were discarded. (d) Some artifacts originate from one or a few distinct sources or a limited volume of space so that the artifact topography is a superposition of characteristic topographies

(equivalently, the artifact is limited to a subspace of the signal space). We removed these artifacts by determining the characteristic topographies (equivalently, the artifact subspace) so that the remaining signals do not contain anything from the artifact subspace. (e) Artifacts and true brain signals that can be assumed to be sufficiently independent can be removed by independent component analysis. (f) Some artifacts are characterized by a particular temporal pattern such as exponential decay. We removed these artifacts by modeling the artifact and fitting its parameters to the data and then removing the artifact.

2.4 | Time windows

The method for calculating dynamic functional connectivity in this study follows the technique used by Zhang et al. (2016) with fMRI data. In their study, they (a) divided the continuous ongoing time series of the BOLD signal into smaller time windows or epochs; (b) calculated the functional connectivity between different brain areas in each epoch and (c) analyzed the pattern of connectivity across different epochs spanning the length of the recording. The windowing procedure itself may be carried out using a window of fixed length (in seconds or minutes) that is shifted by a fixed number of data points across the length of the recording (Hutchison et al., 2013). If the number of data points shifted by is equal to the window length, then epochs with nonoverlapping sliding windows are obtained. However, if the number of data points the window is shifted by is less than the window length, then epochs with overlapping sliding windows are obtained. Dividing the continuous recording into sliding windows can be used to search for the presence of reproducible, transient patterns of region-to-region correlation (“connectivity states”) in both stimulus-evoked and resting activity (Hutchison et al., 2013). In the resting state, subjects are proposed to undergo spontaneous fluctuation in vigilance states that may be reflected in spontaneous fluctuations in connectivity between different brain regions (Hutchison et al., 2013).

In the fMRI literature, it is common to choose windows that are tens of seconds long, given the low temporal resolution of the BOLD signal. However, given the high resolution of EEG data in this study, we chose the smallest window (3 s) for which the software (sLORETA) could reliably calculate functional connectivity between the 84 Brodmann areas in each epoch; this window length was also sufficient to represent the slowest frequency band, that is, delta (2–3.5 Hz). To validate our results, we replicate our analyses using both overlapping and nonoverlapping sliding windows.

After manually cleaning of EEG data, every person had at least 3 min of continuous EEG data. Only the first 3 min of data were used for the people who had more than 3 min of data. The first 15 s of the data were disregarded, and the next 2 min and 45 s of stable EEG recording was considered for

further analysis. The continuous stream of EEG was divided into 3-s epochs of overlapping and nonoverlapping time windows. The overlapping time windows were constructed by shifting (sliding) a 3-s window by 1 s over the length of the recording. The nonoverlapping time windows were constructed by shifting (sliding) the 3-s window by 3 seconds over the length of the recording. This resulted in 163 epochs with overlapping windows and 55 epochs with nonoverlapping windows. We further validated our results with a nonoverlapping window of 5 s to ensure the robustness of our results. This resulted in 33 nonoverlapping windows. The functional connectivity was calculated for the 163 epochs generated using 3-s overlapping windows, 55 epochs generated using 3-s nonoverlapping windows and 33 epochs generated using the 5-s nonoverlapping windows in eight frequency bands as detailed below. Please note that these conditions will henceforth be labeled “overlapping windows”, “nonoverlapping windows” and “nonoverlapping (5 s) windows”, respectively.

2.5 | Source localization

Neuronal activity from the 19 scalp electrodes was localized to 84 intracerebral electrical sources using the standardized low-resolution brain electromagnetic tomography (sLORETA; Pascual-Marqui, 2002) software in each epoch in the three window conditions. The neuronal activity or current density (A/m^2) may be computed using sLORETA without assuming a predefined number of active sources. A common average reference transformation was performed prior to the application of the source localization algorithm (Pascual-Marqui, 2002). The solution space for the algorithm used in this study along with the lead field matrix were implemented in the LORETA-Key software (freely available at: <http://www.uzh.ch/keyinst/loreta.htm>). This software implements the standard electrode positions from the MNI 152 scalp (Jurcak, Tsuzuki, & Dan, 2007) and the lead field produced by Fuchs, Kastner, Wagner, Hawes, and Ebersole (2002) to apply the boundary element method on the T1-weighted MNI-152 (Montreal Neurological Institute, Canada) template (Mazziotta et al., 2001). Thus, the sLORETA-key anatomical template divides and labels neocortical (including hippocampus and anterior cingulate cortex) MNI volume into 6,239 voxels having 5 mm^3 thickness based on probabilities returned by the Talairach Daemon Atlas (Lancaster et al., 2000). The coregistration makes use of the correct translation from the MNI-152 space into the Lancaster et al. (2000) space (Brett, Johnsrude, & Owen, 2002). The 6,239 voxels were distributed into 84 Brodmann areas, which form the regions of interest in this study. The position of the Brodmann areas used is shown in Figure 1 and the abbreviations are expanded in Table 1. The following analyses were performed in eight frequency bands defined as delta (2–3.5 Hz), theta (4–7.5 Hz), alpha1 (8–10 Hz), alpha2

(10–12 Hz), beta1 (13–18 Hz), beta2 (18.5–21 Hz), beta3 (21.5–30 Hz) and gamma (30.5–44 Hz) for the overlapping and nonoverlapping windows. These frequency bands were selected based on previous literature (Vanneste & De Ridder, 2016; Vanneste, van de Heyning, & De Ridder, 2011). The results for the nonoverlapping (5 s) windows were validated in the same frequency bands, except that the alpha1 and alpha2 frequency bands were separated by 0.5 Hz, that is, alpha2 (10.5–12 Hz).

2.6 | Lagged phase coherence – measure of functional connectivity

“Lagged phase coherence” between sources was interpreted as the amount of cross-talk between the regions contributing to the activity within the sources (Congedo, John, De Ridder, Prichep, & Isenhardt, 2010). The cross-talk between the sources was equivalent to the information shared by axonal transmission. In other words, when the signal was decomposed using Fourier decomposition, it segregated into a finite series of sine and cosine waves characterizing the in-phase and out-of-phase carrier waves, thus forming the real and imaginary parts of the decomposition. The magnitude was normalized across the sine and cosine parts and only phase information was considered while calculating lagged phase coherence (Pascual-Marqui et al., 2011). The lag of the cosine waves behind their respective sine counterparts was inversely proportional to their frequency and accounts to a quarter of the period. For example, the period of a sinusoidal wave at 10 Hz is 100 ms. The cosine is shifted a quarter of a cycle (25 ms) with respect to the sine counterpart. This would mean that the lagged phase coherence at 10 Hz indicates coherent oscillations with a 25 ms delay. The same at 20 Hz would indicate a delay of 12.5 ms, etc. The overall phase coherence between the time series of any two Brodmann areas is obtained by computing the cross-spectral matrices. The lagged phase coherence is calculated by subtracting the instantaneous coherence from the overall phase coherence between the two sources. The mathematical expressions are given in (Pascual-Marqui et al., 2011). Here, the authors explained that instantaneous correlations may represent erroneous values of functional connectivity between sources due to volume conduction of electrical signals by brain tissue. Thus, the lagged phase coherence was proposed to be a more accurate measure of actual physiological functional connectivity.

The lagged phase coherence between each pairwise combination of Brodmann areas signifies their functional connectivity strength. The lagged phase coherence between pairs of 84 Brodmann areas were computed in each of the 163 epochs in the overlapping window condition, 55 epochs in the nonoverlapping window condition and 33 nonoverlapping (5 s) window condition in the two groups in the eight frequency bands defined above. The dynamic functional connectivity

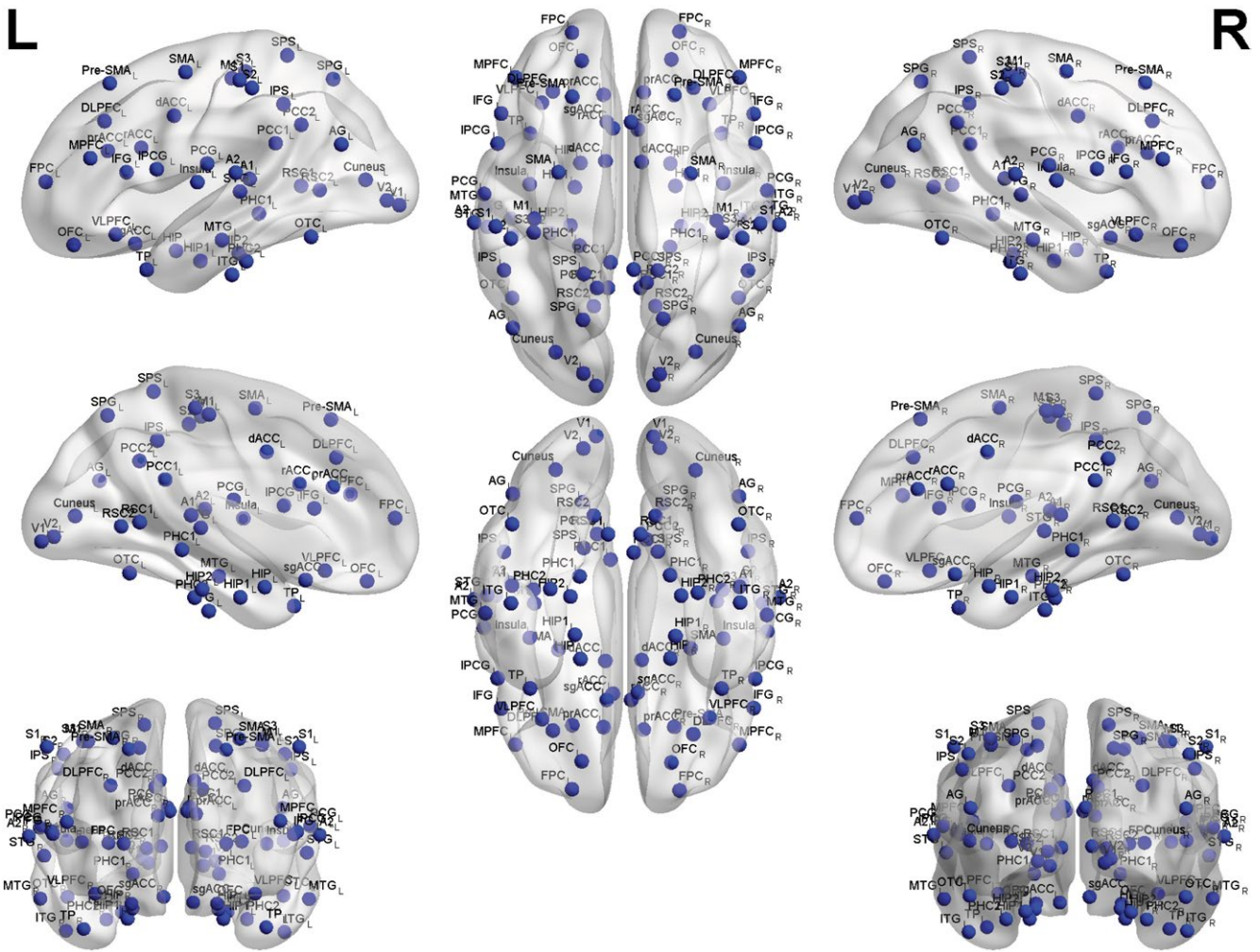


FIGURE 1 The 84 Brodmann areas used in the study

across the 163 overlapping windows in each frequency band is shown as a Videos S1–S8 attached in the Supporting Information. The following analyses were performed in all three windowing conditions.

2.7 | Temporal variability

To analyze the extent to which the pattern of functional connectivity of a node repeats over time (or over epochs), we calculated a measure called temporal variability in accordance with the method published by Zhang et al. (2016) in the three windowing conditions in each frequency band. Thus, temporal variability is the measure of dynamic functional connectivity used in this study. To calculate temporal variability, we defined the term “connectivity vector” as the connectivity strength between a given node and every other node in the network in a given epoch. Hence, for every node k in epoch i , let the connectivity vector be represented as $F_{i,k}$ and for every node k in epoch j , let the connectivity vector be represented as $F_{j,k}$. The connectivity vector of every node in an epoch was correlated with

its corresponding connectivity vector in other epochs. The resultant correlation coefficients were averaged and subtracted from 1 to get temporal variability (Zhang et al., 2016). This is given by the formula,

$$V_k = 1 - \overline{\text{corcoef}(F_{i,k}, F_{j,k})}, i, j = 1, 2, 3, \dots, n, i \neq j$$

where V_k is the temporal variability of node k and n is the number of epochs [$n = 163$ in the overlapping window condition, $n = 55$ in the nonoverlapping window condition and $n = 33$ in the nonoverlapping (5 s) condition]. The temporal variability of all the nodes was averaged to give a network-level measure of temporal variability in each frequency band. The average network-level temporal variability between the two groups in the eight frequency bands was compared using repeated measures analysis of variance (ANOVA) with group as between-subject factor and the eight frequency bands as repeated measures. To compare the temporal variability of each node of the tinnitus group with the control group in each frequency band, a repeated measures ANOVA was performed with group as the

TABLE 1 List of Brodmann areas used in the study

Brodmann areas	Abbreviation	Name of the Brodmann area
BA01	S1	Primary somatosensory cortex
BA02	S2	Secondary somatosensory cortex
BA03	S3	Tertiary somatosensory cortex
BA04	M1	Primary motor cortex
BA05	SPS	Superior parietal sulcus
BA06	SMA	Supplementary motor area
BA07	SPG	Superior parietal gyrus
BA08	Pre-SMA	Presupplementary motor area
BA09	DLPFC	Dorsolateral prefrontal cortex
BA10	FPC	Frontoparietal cortex
BA11	OFC	Orbital frontal cortex
BA13	Insula	Insula
BA17	V1	Primary visual cortex
BA18	V2	Secondary visual cortex
BA19	Cuneus	Cuneus
BA20	ITG	Inferior temporal gyrus
BA21	MTG	Medial temporal gyrus
BA22	STG	Superior temporal gyrus
BA23	PCC1	Posterior cingulate cortex1
BA24	dACC	Dorsal anterior cingulate cortex
BA25	sgACC	Subgenual anterior cingulate cortex
BA27	PHC1	Parahippocampal gyrus1
BA28	HIP1	Hippocampal area1
BA29	RSC1	Retrosplenial cortex1
BA30	RSC2	Retrosplenial cortex2
BA31	PCC2	Posterior cingulate cortex2
BA32	prACC	Pregenual anterior cingulate vortex
BA33	rACC	Rostral anterior cingulate cortex
BA34	HIP	Hippocampus
BA35	HIP2	Hippocampal area2
BA36	PHC2	Parahippocampal gyrus2
BA37	OTC	Occipital temporal cortex
BA38	TP	Temporal pole
BA39	AG	Angular gyrus
BA40	IPS	Intraparietal sulcus
BA41	A1	Primary auditory cortex
BA42	A2	Secondary auditory cortex
BA43	PCG	Postcentral gyrus
BA44	OPCG	Opercular part of inferior frontal gyrus

(Continues)

TABLE 1 (Continued)

Brodmann areas	Abbreviation	Name of the Brodmann area
BA45	IFG	Inferior frontal gyrus
BA46	MPFC	Medial prefrontal cortex
BA47	VLPFC	Ventrolateral prefrontal cortex

between-subject factor and frequency and Brodmann area as repeated measures. Upon observing significant Group x Frequency x Brodmann area interaction, a repeated measures ANOVA was performed at each frequency band with group as the between-subject factor and Brodmann areas as repeated measures. For those frequency bands where we observed a significant Group x Brodmann area interaction, the temporal variability of each node was compared between the two groups using independent *t*-tests to observe the significant differences in temporal variability at every node. The repeated measures ANOVAs were corrected for multiple comparisons using the Bonferroni correction accounting for the number of groups, frequency bands and Brodmann areas and thus the *t*-test between each node was flagged at a *p*-value <0.05. Along with the *F*-values for the ANOVAs, effect size measures such as the Cohen's *d* was also reported for each comparison of temporal variability of the Brodmann areas between the two groups in the eight frequency bands and three window conditions. Cohen's *d* was calculated as the difference between the means of the temporal variability of the two groups divided by the pooled standard deviance. A Cohen's *d* measure of greater than or equal to 0.25 was considered a meaningful effect size measure. These analyses were performed for all three window conditions.

2.8 | Correlation with behavioral data

The network-level measure of temporal variability was partially correlated with the scores on the TQ controlling for age, duration of tinnitus, rating on the VAS for loudness and mean hearing loss in the alpha1 and alpha2 frequency bands. Correlations were flagged as significant if they had a 2-tailed *p* < 0.025 after correcting for the number of frequency bands. The network-level measure of temporal variability was correlated with the scores on the VAS for loudness controlling for age, duration of tinnitus, scores on the TQ, and mean hearing loss in the theta and gamma frequency bands. Correlations were flagged as significant if they had a 2-tailed *p* < 0.025 after correcting for the number of frequency bands.

Tinnitus patients were then subdivided into low- and high-distress tinnitus groups based on their TQ scores. Patients with TQ score ≤46 were classified in the low-distress tinnitus group and patients with TQ score >46 were classified into

the high-distress tinnitus group. These thresholds were based on the clinical classification of different grades of distress in tinnitus: slight (0–30 points; grade 1), moderate (31–46; grade 2), severe (47–59; grade 3) and very severe (60–84; grade 4) distress (Goebel & Hiller, 1994). Thus, patients suffering from grade 1 and grade 2 distress were classified into the low-distress tinnitus group ($N = 91$, $M = 45.30$ years, $SD = 14.30$), patients suffering from grade 3 and grade 4 tinnitus were classified into the high-distress tinnitus group ($N = 45$, $M = 46.71$ years, $SD = 11.35$ years). The network-level measure of temporal variability in the low- and high-distress tinnitus groups was partially correlated with TQ scores in the alpha1 and alpha2 frequency band. Correlations were flagged significant if they had a 2-tailed $p < 0.025$ after correcting for the number of frequency bands. The network-level measure of temporal variability in the low- and high-distress groups was also partially correlated with the scores on the VAS for loudness in the theta, alpha1, alpha2 and gamma frequency bands. Correlations were flagged as significant if they had a 2-tailed $p < 0.013$ after correcting for the number of frequency bands. Further, for those correlations which were significant in the low- or high-distress tinnitus groups, a comparison was made between the correlation coefficients between the two groups to determine if any change in correlation between the low- and high-distress tinnitus groups were statistically significant. This was performed using a linear regression analysis comparing the corresponding steepness of the slopes between the low- and high-distress groups.

2.9 | Region of Interest (ROI) analysis

Correlations between temporal variability and behavioral measures in tinnitus were further investigated at the level of specific regions. The regions of interest were dorsal anterior cingulate cortex (dACC, BA 24), subgenual anterior cingulate cortex (sgACC, BA 25) averaged over left and right regions, bilateral parahippocampus (PHC, BAs 27 and 36) and bilateral primary auditory cortex (A1, BA 41). A1 and the bilateral PHC have been consistently identified as the important regions encoding subjective tinnitus loudness and dACC, sgACC and PHC have been identified as the important regions encoding the emotional component of tinnitus.

The scores on the VAS for loudness were partially correlated with the temporal variability of the bilateral A1 and bilateral PHC in the theta and gamma frequency bands controlling for age, duration of tinnitus, TQ score and mean hearing loss. Correlations were flagged significant if they had a 2-tailed $p < 0.025$ after correcting for the number of frequency bands. The global TQ scores were partially correlated with the temporal variability of dACC, sgACC and PHC in the alpha1 and alpha2 frequency bands controlling for age, duration of tinnitus, TQ score and mean hearing loss. Correlations were flagged significant if they

had a 2-tailed $p < 0.025$ after correcting for the number of frequency bands.

2.10 | Correlation of VAS for loudness and TQ score with temporal variability in low- and high-distress patients

Temporal variability in the low- and high-distress tinnitus patients at A1 and PHC were partially correlated with the scores on their VAS for loudness in the theta, alpha1, alpha2 and gamma frequency bands. Correlations were flagged significant if they had a 2-tailed $p < 0.013$ after correcting for the number of frequency bands. The temporal variability of the low- and high-distress tinnitus patients in the dACC, sgACC and PHC was also partially correlated with the TQ score in the alpha1 and alpha2 frequency bands. Correlations were flagged as significant if they had a 2-tailed $p < 0.025$ after correcting for the number of frequency bands. Furthermore, for those correlations in specific regions of interest that were significant in the low- or high-distress tinnitus groups, a comparison was made between the two groups to determine if any changes in correlation coefficient between the low- and high-distress tinnitus groups were statistically significant. This was performed using a linear regression analysis comparing the corresponding steepness of the slopes between the two groups.

3 | RESULTS

3.1 | Temporal variability – network and nodal level

At the network level, no significant Group \times Frequency interaction was observed for the overlapping ($F(7, 1918) = 2.34$, $p = 0.068$), nonoverlapping ($F(7, 1918) = 2.20$, $p = 0.082$) or nonoverlapping (5sec) ($F(7, 1918) = 1.93$, $p = 0.117$) window conditions. However, a significant group effect was observed for the average temporal variability in the overlapping ($F(1, 274) = 20.77$, $p < 0.001$; Cohen's $d = 0.298$) (Figure 2a), nonoverlapping ($F(1, 274) = 21.44$, $p < 0.001$; Cohen's $d = 0.305$) (Figure 2b) and nonoverlapping (5sec) ($F(1, 274) = 16.86$, $p < 0.001$; Cohen's $d = 0.286$) (Supporting Information Figure S1) window conditions. In all three conditions, we observed that the temporal variability of the tinnitus group was significantly greater than the temporal variability of the control group.

We observed a significant Group \times Brodmann area \times Frequency interaction in the overlapping ($F(581, 159194) = 7.66$, $p < 0.001$), nonoverlapping ($F(581, 159194) = 7.78$, $p < 0.001$) and nonoverlapping (5 s) ($F(581, 159194) = 6.53$, $p < 0.001$) window conditions. In the overlapping window condition, we further observed a significant Group \times Brodmann area interaction in

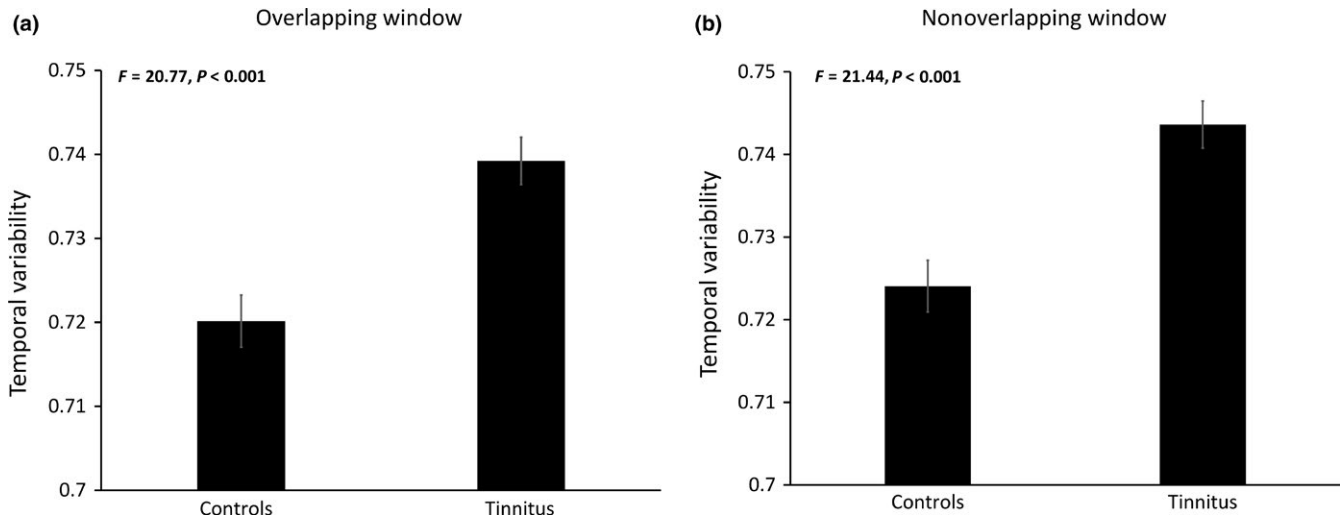


FIGURE 2 Comparison of average temporal variability between the controls and tinnitus groups at the network level in the (a) overlapping window and (b) nonoverlapping window conditions

the delta ($F(83, 22742) = 8.50, p < 0.001$), theta ($F(83, 22742) = 5.99, p < 0.001$), alpha1 ($F(83, 22742) = 6.14, p < 0.001$), alpha2 ($F(83, 22742) = 5.77, p < 0.001$), beta1 ($F(83, 22742) = 5.78, p < 0.001$), beta2 ($F(83, 22742) = 4.72, p < 0.001$), beta3 ($F(83, 22742) = 5.801, p < 0.001$) and gamma ($F(83, 22742) = 14.45, p < 0.001$) frequency bands. Likewise, in the nonoverlapping window condition, we observed a significant Group \times Brodmann area interaction in the delta ($F(83, 22742) = 8.36, p < 0.001$), theta ($F(83, 22742) = 5.71, p < 0.001$), alpha1 ($F(83, 22742) = 6.27, p < 0.001$), alpha2 ($F(83, 22742) = 5.19, p < 0.001$), beta1 ($F(83, 22742) = 5.73, p < 0.001$), beta2 ($F(83, 22742) = 4.39, p < 0.001$), beta3 ($F(83, 22742) = 5.87, p < 0.001$) and gamma ($F(83, 22742) = 14.10, p < 0.001$) frequency bands. At last, in the nonoverlapping (5 s) window condition, we observe a significant Group \times Brodmann area interaction in the delta ($F(83, 22742) = 8.19, p < 0.001$), theta ($F(83, 22742) = 5.83, p < 0.001$), alpha1 ($F(83, 22742) = 6.79, p < 0.001$), alpha2 ($F(83, 22742) = 5.28, p < 0.001$), beta1 ($F(83, 22742) = 4.88, p < 0.001$), beta2 ($F(83, 22742) = 4.25, p < 0.001$), beta3 ($F(83, 22742) = 5.66, p < 0.001$) and gamma ($F(83, 22742) = 14.03, p < 0.001$) frequency bands. The Cohen's d effect size measure for the comparison between controls and tinnitus group for each Brodmann area in each frequency band for the three window conditions is given in Supporting Information Tables S1–S3. At the nodal level, we observed a spatially distributed difference in temporal variability between the control and tinnitus groups. In the overlapping window condition, we observed that the variability in the tinnitus network was significantly greater than the controls mostly in the anterior parts of the cingulum, medial prefrontal regions, parts of the occipital lobe in almost all the frequency bands, most parts of the temporal and medial temporal lobe in alpha1 and alpha2, most of

the frontal cortex in the alpha1 and alpha2 frequency bands, and most of the parietal regions in the beta3 and gamma frequency bands. Regions such as the temporal-parietal junction in the delta frequency band, the inferior temporal gyrus in the beta2, beta3, most of the temporal lobe in gamma, and parts of the medial temporal lobe in the beta1, beta2, beta3 and gamma frequency bands showed significantly decreased variability in the tinnitus network. Regions covering the frontal and prefrontal cortex in all frequencies except the alpha1 and alpha2 frequency bands, the posterior cingulate cortex in all frequencies and parts of the temporal lobe in the alpha1, beta1, beta2 and beta3 bands showed no significant differences in temporal variability (Figure 3). We observed a similar pattern in the nonoverlapping and nonoverlapping (5 s) window conditions, as well (Figure 4, Supporting Information Figure S2).

3.2 | Correlation of network-level temporal variability with VAS for loudness and TQ score

No significant correlations were observed between the VAS for loudness and the network-level temporal variability in the theta or gamma frequency bands in the overlapping, nonoverlapping, or nonoverlapping (5 s) window conditions. No significant correlations were observed between the TQ score and the network-level temporal variability in the alpha1 and alpha2 frequency bands within the overlapping, nonoverlapping, or nonoverlapping (5 s) window condition. All correlation coefficients and their corresponding p -values are reported in Table 2 and Supporting Information Table S4.

When the tinnitus group was divided into low- and high-distress tinnitus groups, no significant correlations were observed between the VAS for loudness and network-level

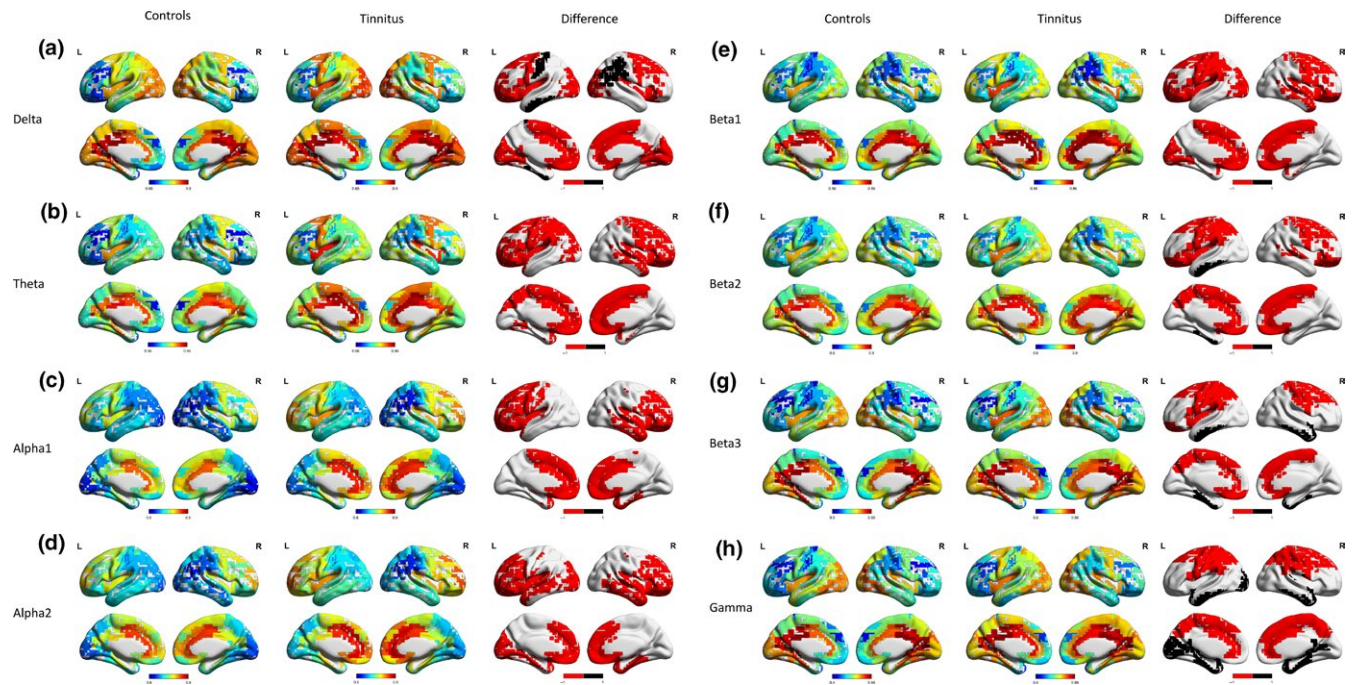


FIGURE 3 Comparison of temporal variability between controls (left panel) and tinnitus (middle panel) at the nodal level in the (a) delta, (b) theta, (c) alpha1, (d) alpha2, (e) beta1, (f) beta2, (g) beta3 and (h) gamma frequency bands in the overlapping window condition. The right-most panel shows the significant differences between the temporal variability in controls and tinnitus. Areas in black denote significantly greater variability in controls, areas in red denote significantly greater variability in tinnitus, and areas in white denote no significant difference between the two groups

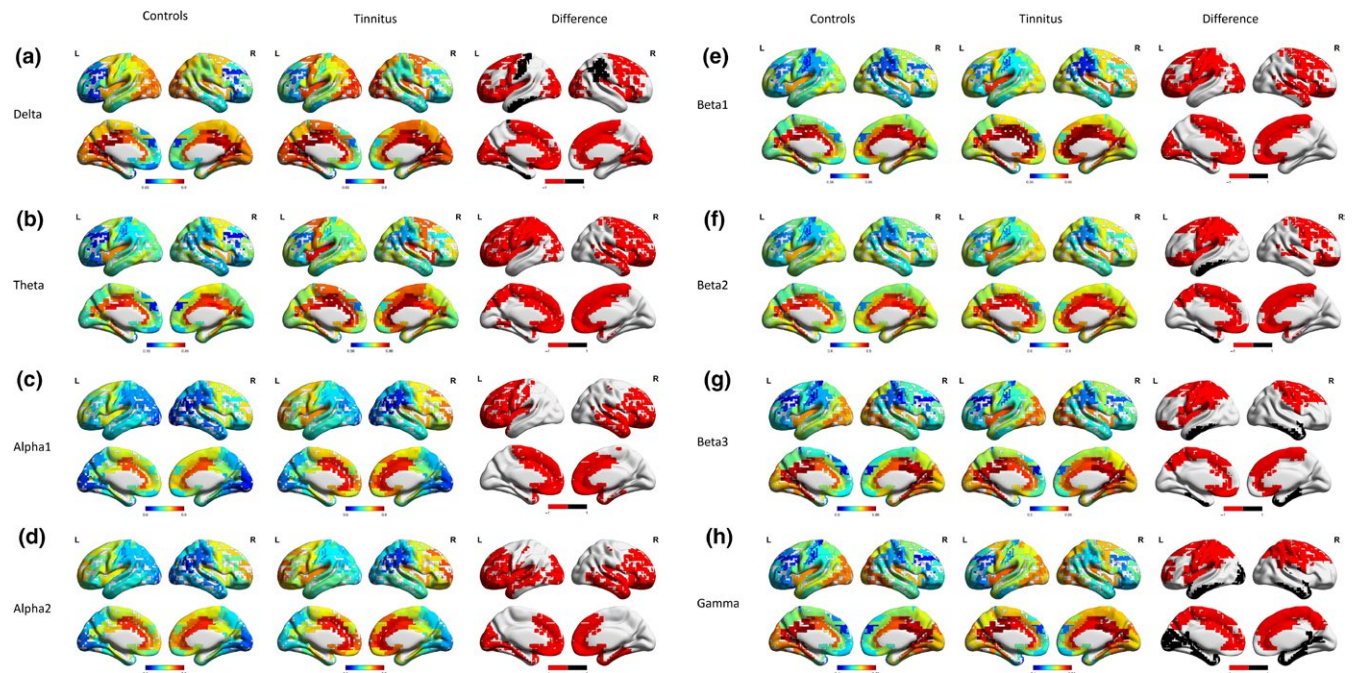


FIGURE 4 Comparison of temporal variability between controls (left panel) and tinnitus (middle panel) at the nodal level in the (a) delta, (b) theta, (c) alpha1, (d) alpha2, (e) beta1, (f) beta2, (g) beta3 and (h) gamma frequency bands in the nonoverlapping window condition. The right-most panel shows the significant differences between the temporal variability in controls and tinnitus. Areas in black denote significantly greater variability in controls, areas in red denote significantly greater variability in tinnitus, and areas in white denote no significant difference between the two groups

TABLE 2 Partial correlation of VAS for loudness and TQ with network-level variability in overlapping and nonoverlapping window conditions in the gamma ($p < 0.025$), alpha1 and alpha2 frequency bands ($p < 0.025$) respectively

Condition	Areas	VAS for loudness	TQ score
Overlapping window condition	Theta	$r = 0.13$ $p = 0.354$	
	Alpha1		$r = -0.09$ $p = 0.511$
	Alpha2		$r = -0.01$ $p = 0.947$
	Gamma	$r = 0.09$ $p = 0.549$	
Nonoverlapping window condition	Theta	$r = 0.11$ $p = 0.433$	
	Alpha1		$r = -0.09$ $p = 0.521$
	Alpha2		$r = -0.02$ $p = 0.907$
	Gamma	$r = 0.11$ $p = 0.456$	

temporal variability for the low- or high-distress tinnitus groups in the theta or gamma frequency bands in any of the three conditions. With respect to the two alpha frequency bands, we observed no significant correlation between VAS for loudness and network-level temporal variability for the low-distress tinnitus group. However, for high-distress tinnitus group, we observed a strong positive correlation in the alpha1 and alpha2 frequency bands in each of the three window conditions (Figures 5a,b and 6a,b, Supporting Information Figures S3a, S4a, S5a,b). Furthermore, in the overlapping window condition, a significant difference between the correlation coefficients of the low- and high-distress tinnitus group was observed in the alpha1 ($t = 2.04$, $p = 0.046$) and alpha2 ($t = 2.64$, $p = 0.011$) frequency bands (Supporting Information Figure 3b). In the nonoverlapping window condition, a marginally significant difference was observed between the correlation coefficients of the low- and high-distress tinnitus groups in the alpha1 frequency band ($t = 1.99$, $p = 0.052$) and a significant difference was observed in the alpha2 frequency band ($t = 2.34$, $p = 0.023$) (Supporting Information Figure 3b). In the nonoverlapping (5 s) window condition, a significant difference was observed between the correlation coefficients of the low- and high-distress tinnitus groups in the alpha1 frequency band ($t = 2.09$, $p = 0.042$) but not in the alpha2 frequency band ($t = 1.93$, $p = 0.058$; Supporting Information Figure 4b). All

correlation coefficients and their corresponding p -values are reported in Table 3 and Supporting Information Table S5.

With respect to the TQ score, we observed no significant correlation between TQ score and the network-level temporal variability in the low- and high-distress tinnitus group in the alpha1 frequency band in any of the windowing conditions. In the alpha2 frequency band, we observed no significant correlation between the TQ score and network-level temporal variability in the low-distress tinnitus group. However, we observed a significant negative correlation in the high-distress tinnitus group in the overlapping and nonoverlapping window conditions (Figures 5c and 6c, Supporting Information Figure 3c) but not in the nonoverlapping (5 s) window condition (Supporting Information Figures S4a, S5c). Furthermore, in the overlapping window condition, a significant difference between the correlation coefficients of the low- and high-distress tinnitus group was observed in the alpha2 ($t = -2.92$, $p = 0.005$) frequency band (Supporting Information Figure 3d). This trend was not observed in the nonoverlapping window condition ($t = -1.94$, $p = 0.058$; Supporting Information Figure 3d). All the correlation coefficients along with their p -values are given in Table 3 and Supporting Information Table S5.

3.3 | Correlation of ROI level variability with VAS for loudness and TQ score

We observed no significant correlations between temporal variability and VAS for loudness or TQ score in any of the regions of interest for the theta, gamma, alpha1 or alpha2 frequency bands in the overlapping, nonoverlapping or nonoverlapping (5 s) window conditions. All correlation coefficients and p -values are reported in Tables 4 and 5 and Supporting Information Tables S6 and S7.

When the tinnitus group was divided into low- and high-distress tinnitus groups, no significant correlation was observed between VAS for loudness and temporal variability of the bilateral PHC and A1 for either groups in the theta or gamma frequency bands in the overlapping, nonoverlapping or nonoverlapping (5 s) window conditions. In the alpha1 and alpha2 frequency bands, we observed no significant correlation between VAS for loudness and temporal variability of the bilateral PHC and A1 in the low-distress tinnitus group in all the conditions. However, we observed a strong, positive relationship between the two variables in the bilateral PHC in the alpha1 and alpha2 frequency bands, in the left A1 in the alpha1 frequency band, and in the right A1 in the alpha2 frequency band in the high-distress tinnitus group. This trend is common to the overlapping and nonoverlapping window conditions (Figures 7a,b and 8a,b, Supporting Information Figures S6a, S7a, S8a,b). We also observed a marginally significant yet strong positive correlation in the alpha1 frequency band in the right A1 in the nonoverlapping window

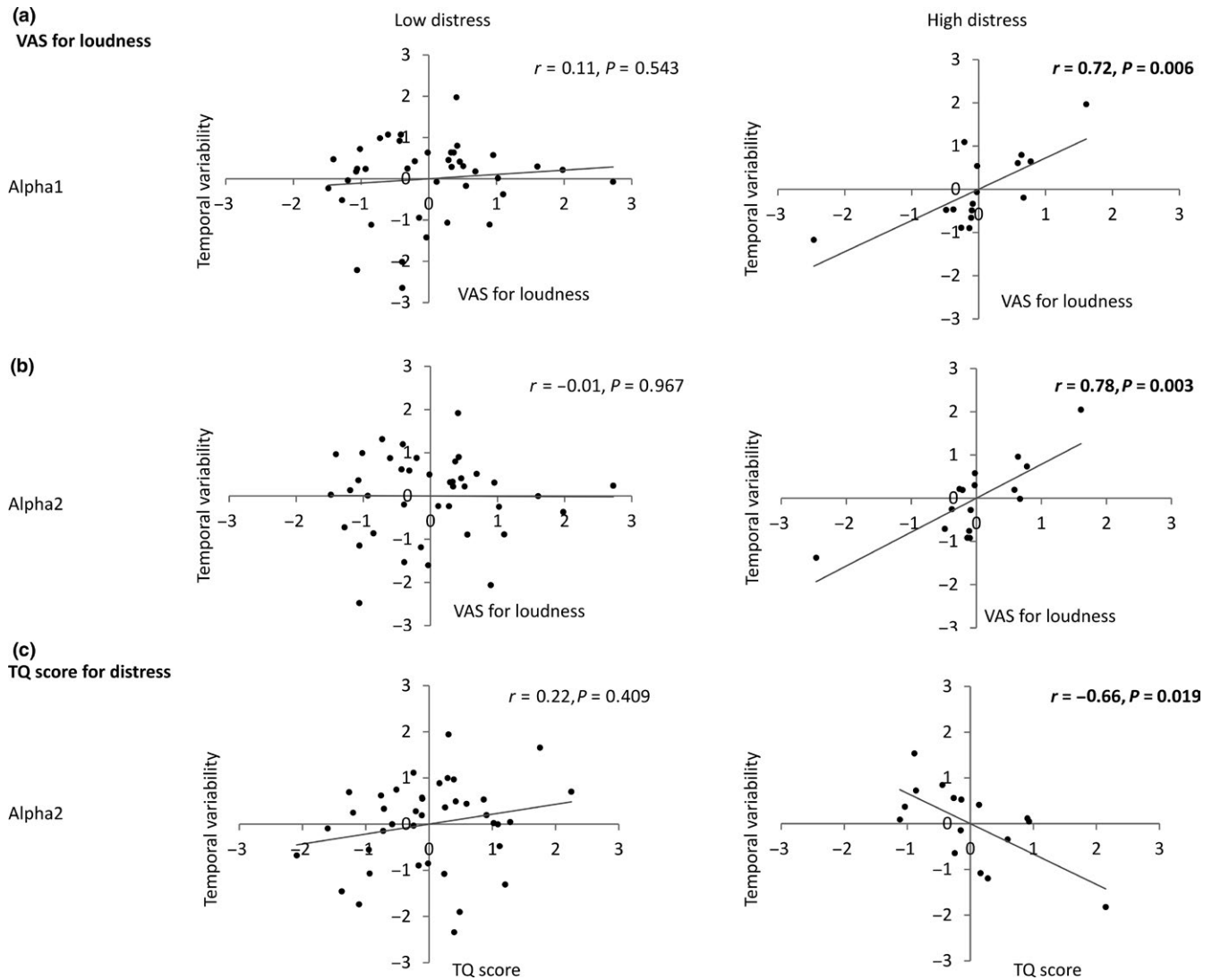


FIGURE 5 Scatter plots for correlation of network-level temporal variability with VAS for loudness and TQ score in low- and high-distress groups in the overlapping window condition. (a) represents the scatter plot for partial correlation of VAS for loudness with network-level temporal variability for low- and high-distress groups in the alpha1 frequency band. (b) represents the scatter plot for partial correlation of VAS for loudness with network-level temporal variability for low- and high-distress groups in the Alpha2 frequency band. (c) represents the scatter plot for partial correlation of TQ score with network-level temporal variability for low- and high-distress groups in the Alpha2 frequency band

condition. In the nonoverlapping (5sec) window condition, we observed a significant and strong positive correlation between the VAS for loudness and temporal variability of the left PHC in the alpha1 and alpha2 frequency bands and the right PHC only in the alpha2 frequency band for the high-distress group (Supporting Information Figures S7a, S8a,b). In the same way, we observed a marginally significant yet strong positive correlation between the temporal variability of the left A1 and VAS for loudness in the alpha1 frequency band and a significant strong positive correlation was also observed for the right A1 in the alpha2 frequency band. All correlation coefficients are reported in Table 4 and Supporting Information Table S6.

In the overlapping window condition, a significant difference in the correlation between VAS for loudness and

temporal variability between the low- and high-distress tinnitus groups was observed for the left PHC in the alpha1 ($t = 2.93, p = 0.005$) and alpha2 ($t = 3.24, p = 0.002$) frequency bands and for the right PHC in the alpha2 ($t = 2.29, p = 0.016$) frequency band (Supporting Information Figure 6b). No significant difference in the correlation coefficient between the low- and high-distress tinnitus groups was observed for the right PHC in the alpha1 ($t = 1.95, p = 0.056$) frequency band. A significant difference in the correlation coefficient between the low- and high-distress tinnitus groups was also observed for the left A1 ($t = 2.50, p = 0.016$) in the alpha1 frequency band. No significant difference between the correlation coefficients was observed between the low- and high-distress groups for the right A1 in the alpha2 frequency band ($t = 1.79, p = 0.079$).

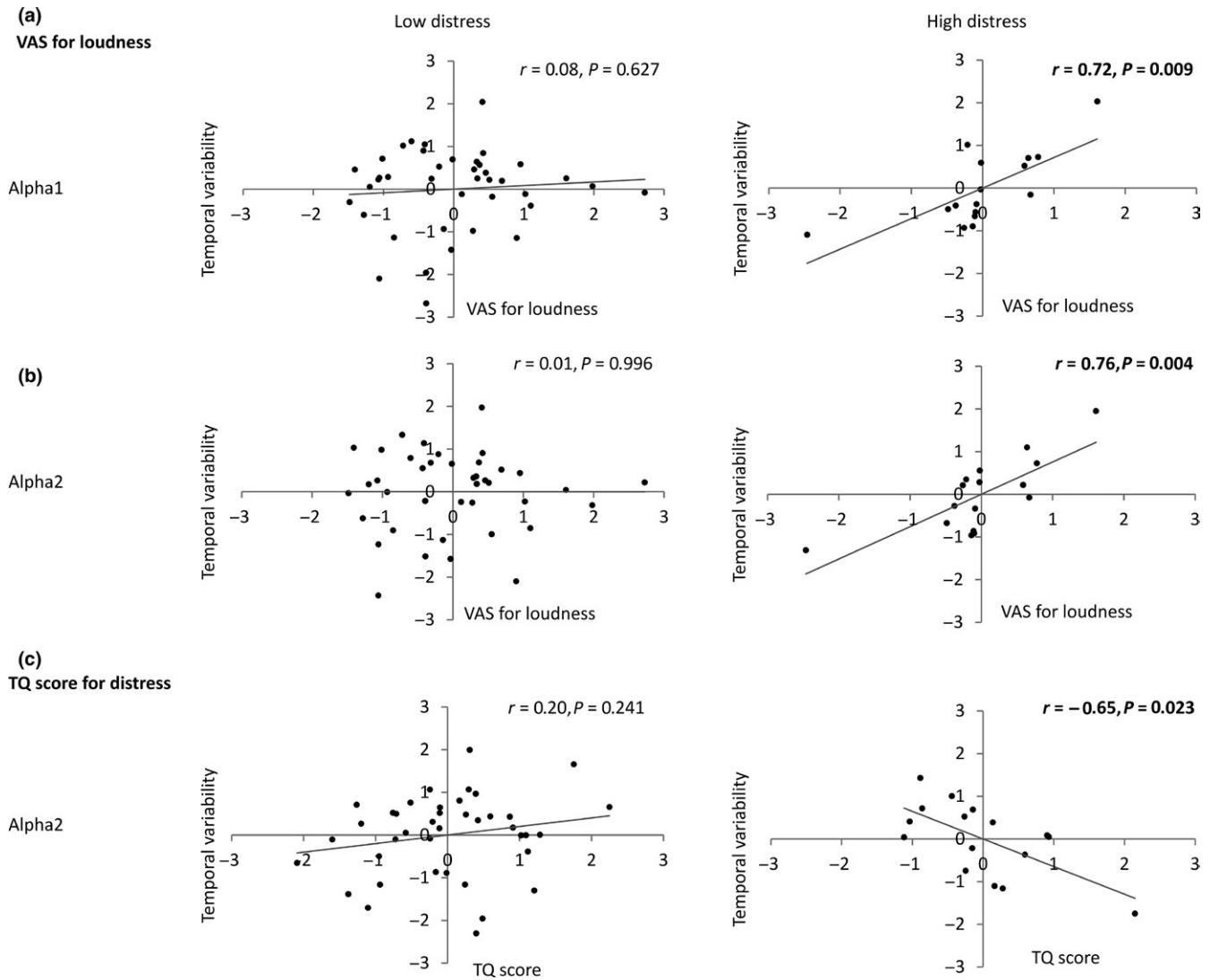


FIGURE 6 Scatter plots for correlation of network-level temporal variability with VAS for loudness and TQ score in low- and high-distress groups in the nonoverlapping window condition. (a) represents the scatter plot for partial correlation of VAS for loudness with network-level temporal variability for low- and high-distress groups in the Alpha1 frequency band. (b) represents the scatter plot for partial correlation of VAS for loudness with network-level temporal variability for low- and high-distress groups in the Alpha2 frequency band. (c) represents the scatter plot for partial correlation of TQ score with network-level temporal variability for low- and high-distress groups in the Alpha2 frequency band

In the nonoverlapping window condition, a significant difference in the correlation coefficients between VAS for loudness and temporal variability between the low- and high-distress tinnitus groups was observed for the left PHC in the alpha1 ($t = 2.88, p = 0.006$) and alpha2 ($t = 2.84, p = 0.008$) frequency bands and right PHC in the alpha2 ($t = 2.48, p = 0.017$) frequency band (Supporting Information Figure 6b). No significant difference in the correlation coefficient between the low- and high-distress tinnitus groups was observed for the right PHC in the alpha1 ($t = 2.01, p = 0.049$) frequency band. A significant difference in the correlation coefficient between the low- and high-distress tinnitus groups was also observed for the left ($t = 2.38, p = 0.021$) and right ($t = 2.21, p = 0.032$) A1 in alpha1 frequency band. No significant difference between the correlation coefficients was observed

between the low- and high-distress tinnitus groups for the right A1 in the alpha2 frequency band ($t = 1.82, p = 0.075$).

In the nonoverlapping (5 s) window condition, a significant difference in the correlation coefficients of VAS for loudness and temporal variability between the low-distress and high-distress tinnitus groups was observed for the left PHC in the alpha1 ($t = 2.32, p = 0.024$) and alpha2 ($t = 2.57, p = 0.013$) frequency bands but not for the right PHC in the alpha2 frequency band ($t = 1.87, p = 0.067$; Supporting Information Figure 7b). A significant difference in the correlation coefficients of VAS for loudness and temporal variability between the low- and high-distress groups was also observed for the left A1 ($t = 2.23, p = 0.03$) in the alpha1 frequency band but not for the right A1 ($t = 1.71, p = 0.094$) in the alpha2 frequency band.

TABLE 3 Correlation of VAS for loudness and TQ score with temporal variability in low and high distress in the gamma, alpha1 and alpha2 ($p < 0.013$) and alpha1 and alpha2 frequency bands, respectively ($p < 0.025$). p -Values in BOLD determine significant correlations after correction for multiple comparison

Condition	Areas	VAS for loudness		TQ score	
		Low distress	High distress	Low distress	High distress
Overlapping window condition	Theta	$r = 0.10$	$r = 0.24$		
		$p = 0.562$	$p = 0.451$		
	Alpha1	$r = 0.11$	$r = \mathbf{0.72}$	$r = 0.09$	$r = -0.36$
		$p = 0.543$	$p = \mathbf{0.006}$	$p = 0.588$	$p = 0.246$
	Alpha2	$r = -0.01$	$r = \mathbf{0.78}$	$r = 0.22$	$r = -\mathbf{0.66}$
		$p = 0.967$	$p = \mathbf{0.003}$	$p = 0.409$	$p = \mathbf{0.019}$
	Gamma	$r = 0.06$	$r = 0.20$		
		$p = 0.709$	$p = 0.544$		
Nonoverlapping window condition	Theta	$r = 0.07$	$r = 0.27$		
		$p = 0.693$	$p = 0.390$		
	Alpha1	$r = 0.08$	$r = \mathbf{0.72}$	$r = 0.09$	$r = -0.24$
		$p = 0.627$	$p = \mathbf{0.009}$	$p = 0.590$	$p = 0.283$
	Alpha2	$r = -0.01$	$r = \mathbf{0.76}$	$r = 0.20$	$r = -\mathbf{0.65}$
		$p = 0.996$	$p = \mathbf{0.004}$	$p = 0.241$	$p = \mathbf{0.023}$
	Gamma	$r = 0.08$	$r = 0.25$		
		$p = 0.636$	$p = 0.429$		

With respect to TQ, no significant relationship between TQ score and temporal variability was observed in the dACC and sgACC for the low- or high-distress tinnitus groups in alpha1 or alpha2 frequency bands in all window conditions. Although there was no significant relationship between TQ score and temporal variability in the low-distress tinnitus group, we observed a strong, negative relationship in the high-distress tinnitus group for the bilateral PHC in the alpha2 frequency consistent for the overlapping and non-overlapping windowing conditions (Figures 7c,d and 8c,d, Supporting Information Figure 6c). This effect was however not observed in the nonoverlapping (5 s) window condition (Supporting Information Figure 8c,d). Furthermore, in the overlapping window condition, a significant difference between the correlation coefficients of the low- and high-distress tinnitus group was observed for the left PHC ($t = -2.18$, $p = 0.034$) and right PHC ($t = -2.28$, $p = 0.027$) in the alpha2 frequency band (Supporting Information Figure 6d). In the nonoverlapping window condition, no significant difference between the correlation coefficients of the two groups was observed in the left PHC ($t = -1.87$, $p = 0.068$). However, a significant difference between the correlation coefficients between the two groups was observed for the right PHC in the alpha2 frequency band ($t = -2.23$, $p = 0.030$) (Supporting Information Figure 6d). All correlation coefficients and their corresponding p -values are reported in Table 5 and Supporting Information Table S7.

4 | DISCUSSION

The aim of the current study is to understand the pathophysiological and symptomatic changes in temporal variability of brain regions in patients perceiving a phantom sound. This is demonstrated using a measure assessing the average epoch-to-epoch correlation of functional connectivity as computed by lagged phase synchronization of a node with other nodes over the entire stretch of the recording. The greater the correlation, the lesser the temporal variability of a node. This measure of temporal variability is inspired by the fMRI literature (Zhang et al., 2016), where the authors describe a topographical way for looking at temporal changes in functional connectivity. The methods used in the current study are different from older methods such as calculating temporal correlations of amplitude fluctuations to examine temporal variability of EEG data. The drawback in using amplitude fluctuations to calculate functional connectivity between cortical sources is that it could be biased by volume conduction of the head (Pascual-Marqui, 2007). Thus, to investigate the topographical change in temporal variability of functional connectivity at the cortical level in tinnitus using EEG data, we used lagged phase coherence and this method inspired from fMRI literature.

The temporal variability of all the nodes is averaged to obtain a whole-brain measure of temporal variability and

TABLE 4 Partial correlation of VAS for loudness with variability at specific nodes in the overlapping and nonoverlapping window conditions in the theta and gamma frequency band ($p < 0.025$) and in the low- and high-distress patients in the alpha1 and alpha2 frequency bands ($p < 0.013$). p -Values in BOLD determine significant correlations after correction for multiple comparison

Condition	Areas	Theta		Alpha1		Alpha2		Gamma	
		All subjects	All subjects	Low distress	High distress	Low distress	High distress	Low distress	High distress
Overlapping window condition	Left PHC	$r = 0.16$	$r = 0.14$	$r = 0.01$	$r = 0.64$	$r = 0.05$	$r = 0.83$	$r = -0.15$	$r = 0.89$
		$p = 0.268$	$p = 0.321$	$p = 0.937$	$p = 0.025$	$p = 0.790$	$p = 0.001$	$p = 0.383$	$p < 0.001$
	Right PHC	$r = -0.03$	$r = 0.05$	$r = -0.13$	$r = 0.31$	$r = 0.21$	$r = 0.78$	$r = 0.07$	$r = 0.85$
		$p = 0.818$	$p = 0.736$	$p = 0.448$	$p = 0.322$	$p = 0.215$	$p = 0.003$	$p = 0.681$	$p < 0.001$
	Left A1	$r = 0.14$	$r = 0.13$	$r = 0.04$	$r = 0.58$	$r = -0.10$	$r = 0.73$	$r = -0.21$	$r = 0.64$
		$p = 0.342$	$p = 0.363$	$p = 0.832$	$p = 0.050$	$p = 0.547$	$p = 0.007$	$p = 0.225$	$p = 0.024$
	Right A1	$r = -0.01$	$r = -0.08$	$r = -0.12$	$r = 0.08$	$r = 0.12$	$r = 0.67$	$r = 0.05$	$r = 0.83$
		$p = 0.937$	$p = 0.558$	$p = 0.499$	$p = 0.793$	$p = 0.505$	$p = 0.017$	$p = 0.781$	$p = 0.001$
Nonoverlapping window condition	Left PHC	$r = 0.13$	$r = 0.15$	$r = -0.04$	$r = 0.68$	$r = 0.05$	$r = 0.82$	$r = -0.11$	$r = 0.82$
		$p = 0.358$	$p = 0.279$	$p = 0.826$	$p = 0.015$	$p = 0.785$	$p = 0.001$	$p = 0.525$	$p = 0.001$
	Right PHC	$r = -0.02$	$r = 0.06$	$r = -0.12$	$r = 0.39$	$r = 0.17$	$r = 0.77$	$r = 0.07$	$r = 0.85$
		$p = 0.888$	$p = 0.655$	$p = 0.471$	$p = 0.210$	$p = 0.310$	$p = 0.003$	$p = 0.683$	$p = 0.001$
	Left A1	$r = 0.12$	$r = 0.16$	$r = 0.03$	$r = 0.53$	$r = -0.09$	$r = 0.72$	$r = -0.18$	$r = 0.56$
		$p = 0.389$	$p = 0.255$	$p = 0.855$	$p = 0.073$	$p = 0.608$	$p = 0.008$	$p = 0.299$	$p = 0.060$
	Right A1	$r = -0.02$	$r = -0.08$	$r = -0.13$	$r = 0.13$	$r = 0.08$	$r = 0.69$	$r = 0.01$	$r = 0.83$
		$p = 0.914$	$p = 0.555$	$p = 0.466$	$p = 0.686$	$p = 0.658$	$p = 0.013$	$p = 0.953$	$p = 0.001$

TABLE 5 Partial correlation of TQ score with variability at specific nodes in the overlapping and nonoverlapping window conditions in the alpha1 and alpha2 frequency bands and in the low- and high-distress patients in the alpha1 and alpha2 frequency bands ($p < 0.025$)

Condition	Areas	Alpha1			Alpha2		
		All subjects	Low distress	High distress	All subjects	Low distress	High distress
Overlapping window condition	dACC	$r = 0.08$	$r = 0.08$	$r = -0.45$	$r = 0.12$	$r = 0.21$	$r = -0.56$
		$p = 0.599$	$p = 0.645$	$p = 0.146$	$p = 0.404$	$p = 0.211$	$p = 0.058$
	sgACC	$r = -0.07$	$r = 0.17$	$r = -0.15$	$r = -0.06$	$r = 0.25$	$r = -0.18$
		$p = 0.631$	$p = 0.327$	$p = 0.639$	$p = 0.686$	$p = 0.140$	$p = 0.586$
	Left PHC	$r = -0.06$	$r = 0.03$	$r = -0.56$	$r = 0.10$	$r = 0.17$	$r = -0.77$
		$p = 0.668$	$p = 0.887$	$p = 0.057$	$p = 0.479$	$p = 0.337$	$p = 0.003^*$
Nonoverlapping window condition	dACC	$r = -0.17$	$r = 0.07$	$r = -0.52$	$r = -0.01$	$r = 0.21$	$r = -0.77$
		$p = 0.218$	$p = 0.692$	$p = 0.081$	$p = 0.947$	$p = 0.220$	$p = 0.003^*$
	sgACC	$r = 0.04$	$r = 0.06$	$r = -0.35$	$r = 0.11$	$r = 0.19$	$r = -0.53$
		$p = 0.789$	$p = 0.726$	$p = 0.263$	$p = 0.457$	$p = 0.271$	$p = 0.074$
	Left PHC	$r = -0.10$	$r = 0.15$	$r = -0.14$	$r = -0.07$	$r = 0.23$	$r = -0.20$
		$p = 0.502$	$p = 0.396$	$p = 0.673$	$p = 0.635$	$p = 0.184$	$p = 0.540$
	Right PHC	$r = -0.04$	$r = 0.01$	$r = -0.53$	$r = 0.11$	$r = 0.13$	$r = -0.60$
		$p = 0.755$	$p = 0.978$	$p = 0.077$	$p = 0.443$	$p = 0.447$	$p = 0.015^*$
		$r = -0.16$	$r = 0.07$	$r = -0.56$	$r = -0.04$	$r = 0.18$	$r = -0.78$
		$p = 0.207$	$p = 0.679$	$p = 0.060$	$p = 0.779$	$p = 0.295$	$p = 0.003^*$

* $p < 0.025$.

this was compared between tinnitus patients and healthy controls. The whole-brain measure of temporal variability is sub-specified for tinnitus patients and with different levels of distress. Then, we looked at specific tinnitus-related nodes and observed that changes in temporal variability of a node in the tinnitus group are spatially distributed and correlated with important behavioral measures such as the loudness of the tinnitus percept and associated distress.

Overall, we observed an increase in temporal variability in tinnitus patients in comparison to healthy controls. This may be attributed to increased flexibility of switching connectivity between different functional modules, thus increasing the number of possible routes for information transfer (Deco & Kringelbach, 2016; Zhang et al., 2016). With respect to pathology, this can be interpreted as a maladaptive compensation by the brain looking for more information in its environment to make up for the loss of sensory input (i.e., auditory deafferentation with or without clinical hearing loss) by rapidly binding with different brain regions (Mohan & Vanneste, 2017).

At the nodal level, we reported spatially distributed patterns of both increases and decreases in temporal variability. On the one hand, we observed an increase in temporal variability in frontal-parietal regions and in different parts of the ACC in all frequency bands. On the other hand, we observed a decrease in temporal variability in the regions of the temporal and medial temporal lobes, mostly in the beta and gamma frequency bands. The increase in variability in the frontal-parietal and

ACC areas may be attributed to an increase in flexibility of connectivity, that is, looking for more information to compensate an elevation in top-down goal-directed salience similar to that observed in patients with depression and schizophrenia (Fecteau & Munoz, 2006; Fox et al., 2005; Kaiser et al., 2015; Zhang et al., 2016). The decreased temporal variability in the regions of the temporal and medial temporal lobe may be reflective of increased temporal synchronization and increased stability of time-varying functional connectivity (Engel & Singer, 2001). Such stable patterns of temporal variability of the medial temporal regions, especially the PHC, may be indicative of focus on self-generated stimuli similar to that demonstrated in patients with depression and schizophrenia (Kaiser et al., 2015; Zhang et al., 2016), or it could reflect an increase in less flexible or less adaptive contextual (distress) influences on the tinnitus loudness perception.

One of the most important and novel findings of this paper is that changes in overall temporal variability is reflected in the symptomatic behavioral characteristics of tinnitus such as loudness of the percept and associated distress. These non-linear changes also depend on the patients' level of distress. We observed that there is no relationship between the temporal variability and distress component in patients who are not very bothered by their tinnitus, but there exists a strong negative correlation in highly distressed tinnitus patients in the alpha2 frequency band. This means that, in highly distressed patients, an increase in predictability or stability of the pattern in functional connectivity in different epochs goes

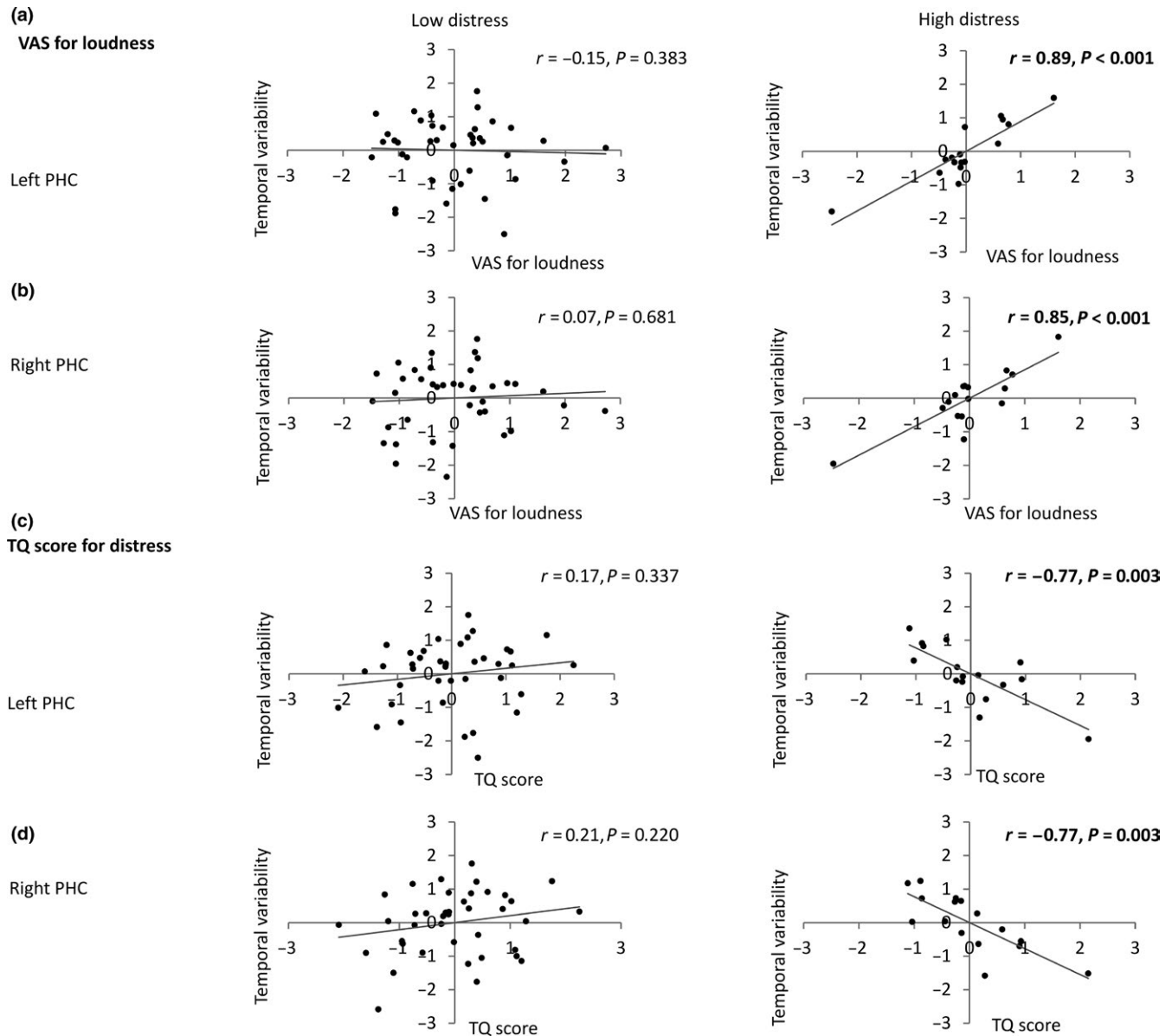


FIGURE 7 Scatter plots for correlation of temporal variability of bilateral PHC with VAS for loudness and TQ score in low- and high-distress groups in the overlapping window condition in the Alpha2 frequency band. (a) represents the scatter plot for partial correlation of VAS for loudness with temporal variability of left PHC for the low- and high-distress groups. (b) represents the scatter plot for partial correlation of VAS for loudness with temporal variability of right PHC for the low- and high-distress groups. (c) represents the scatter plot for partial correlation of TQ score with temporal variability of left PHC for the low- and high-distress groups. (d) represents the scatter plot for partial correlation of TQ score with temporal variability of right PHC for the low- and high-distress groups

together with an increase in the amount of perceived distress. Thus, the networks of highly distressed people are seemingly less dynamic and less flexible and are possibly more hard-wired into that particular state. Behaviorally, this could be a reason for such patients to be extremely focused on their percept (Baguley, Humphriss, & Hodgson, 2000; Zeman et al., 2011). However, people who are not very bothered by their tinnitus do not show such a relationship between changes in temporal variability and tinnitus-related distress, demonstrating a resilience in the dynamic configuration of the network which gives room for change without having an effect on

the amount of perceived distress (Werff, Pannekoek, Stein, & Wee, 2013). The difference in the relationship of temporal variability and perceived distress in the low- and high-distress groups also suggests that there may be a critical point up to which the brain is resilient to changes either in temporal variability or psychological stress, thus keeping the brain flexible and keeping distress levels low. However, once that critical point is reached, the brain becomes less resilient to change and possibly cascades into being more hard-wired in that particular state, possibly leading to high-distress levels (Stark, 2012).

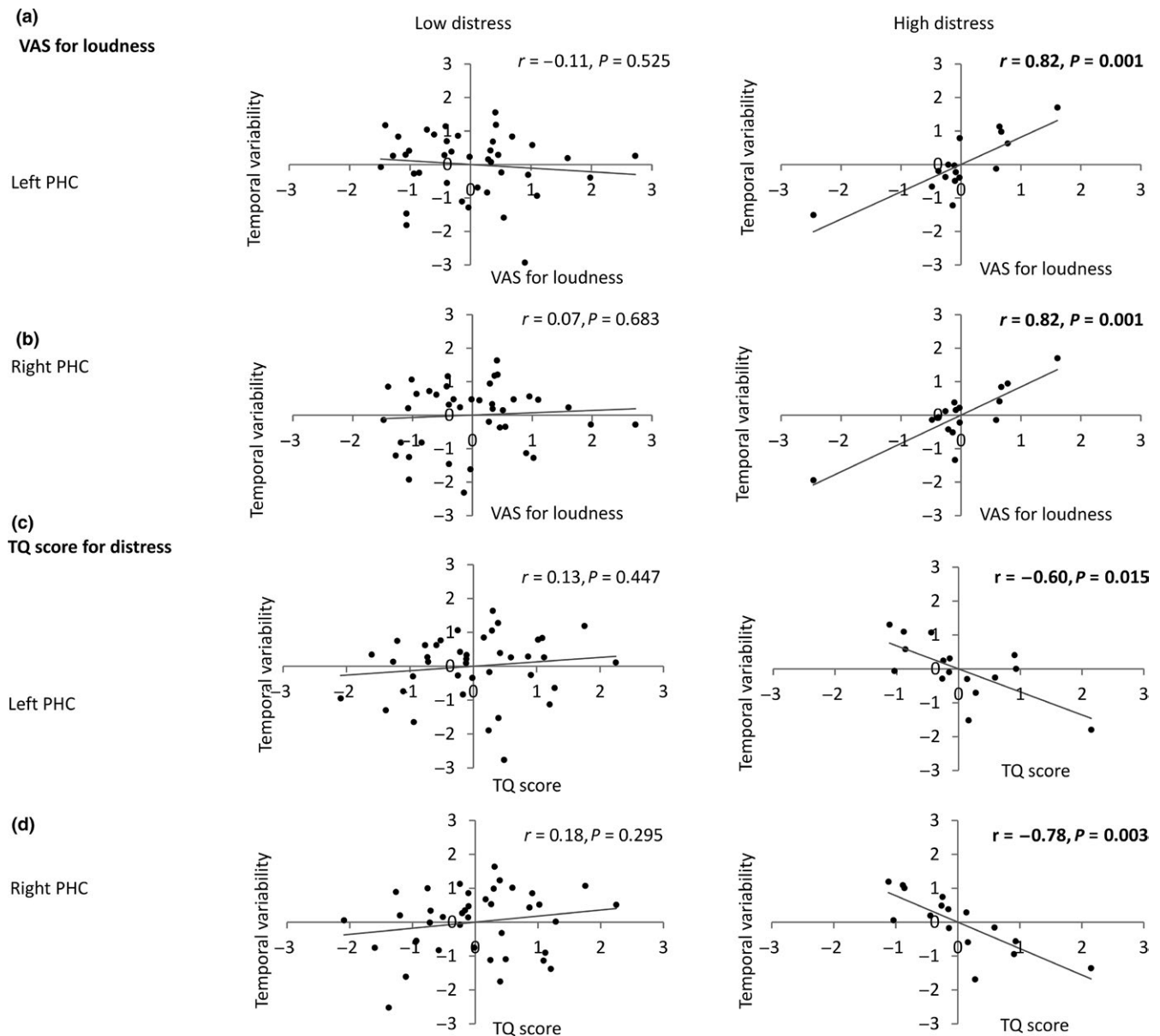


FIGURE 8 Scatter plots for correlation of temporal variability of bilateral PHC with VAS for loudness and TQ score in low- and high-distress groups in the nonoverlapping window condition in the Alpha2 frequency band. (a) represents the scatter plot for partial correlation of VAS for loudness with temporal variability of left PHC for the low- and high-distress groups. (b) represents the scatter plot for partial correlation of VAS for loudness with temporal variability of right PHC for the low- and high-distress groups. (c) represents the scatter plot for partial correlation of TQ score with temporal variability of left PHC for the low- and high-distress groups. (d) represents the scatter plot for partial correlation of TQ score with temporal variability of right PHC for the low- and high-distress groups

This strong negative correlation between temporal variability and perceived distress in highly distressed patients is also observed in the bilateral PHC in the alpha2 frequency band. The PHC plays a significant role in encoding tinnitus-related distress (De Ridder, Vanneste, & Congedo, 2011; Ueyama et al., 2013). The increased alpha activity in the PHC was positively correlated with increasing tinnitus distress (Vanneste et al., 2010). In addition, increased connectivity was observed between the PHC and the deeper structures of the medial temporal lobe such as the amygdala, nucleus accumbens which were also involved in assessing the negative

affect (Maudoux, Lefebvre, Cabay, et al., 2012; Maudoux, A., Lefebvre, P., Cabay, 2012). Complementary to these findings from activity and static connectivity, the decreased temporal variability with increasing distress in highly distressed patients in the PHC further supports the idea that the PHC is involved in dynamically integrating the different regions of the distress network.

On the contrary, we observed a strong positive correlation between temporal variability and the loudness percept in highly distressed patients in the alpha frequency bands both at a network level and ROI level. Increase in gamma activity

in the A1 and increase in functional connectivity with the PHC in the theta frequency band were shown to encode the loudness of the tinnitus percept (De Ridder, Congedo, & Vanneste, 2015; van der Loo et al., 2009). The maladaptive increase in gamma activity in the A1 is hypothesized to reflect the search for compensatory information in mild sensory deafferentation (De Ridder, Vanneste, Langguth, & Llinas, 2015). In severe deafferentation, increased functional connectivity between the A1 and PHC is hypothesized to drive maladaptive compensation by recalling the missing information from the auditory sensory memory (Vanneste & De Ridder, 2016). However, it was shown that this relationship was modulated by changes in functional connectivity between A1 and sgACC in the alpha frequency band (Vanneste & De Ridder, 2015). In the current study, we see that the loudness of the percept increases significantly with increasing temporal variability of the A1 in the alpha frequency band, which may indicate a significant effect of distress in modulating the loudness of the percept. Thus, we demonstrate we also demonstrate that the more rapid the connectivity and search for information, the louder the percept.

In addition to integrating the regions of the distress network, the PHC is known to be a multimodal region that connects the loudness and distress networks via its connection with the sgACC in the alpha frequency band in highly distressed patients (Vanneste et al., 2014). Thus, the difference between low- and high-distress patients was also attributed to the maladaptive association between the loudness and distress networks (Vanneste & De Ridder, 2015; Vanneste et al., 2014). In support of this hypothesis, we first observe that the PHC exhibits a multimodal character by dynamically encoding the loudness and the distress components in the alpha frequency bands in diametrically opposing patterns possibly suggesting a dynamic association between the two networks in highly distressed patients. This finding adds a dynamic aspect to the existing evidence that loudness and distress may be encoded by independent, overlapping subnetworks (De Ridder, Vanneste, Weisz, et al., 2014; Mohan, Moreno, Song, De Ridder, & Vanneste, 2017).

The current study is the first study to our knowledge that investigates the temporal changes in functional connectivity between 84 Brodmann areas in tinnitus and provides a relationship with corresponding behavioral tinnitus. Such a biomarker for dynamic network reconfiguration is crucial to understanding the underlying dynamics of tinnitus network especially during the time when researchers are interested in investigating ways to modify brain regions and networks. We further observe that depending on the amount of distress, the pattern of network connectivity becomes more stable and hence predictable over 3 minutes of resting brain activity, suggesting that such hard-wiring of the network may be the reason why tinnitus is extremely difficult to treat.

Although we investigated tinnitus in particular, the results of the current study could be very critical in understanding some fundamental dynamics of brain regions. We observe that sensory deafferentation changes the dynamics of both unimodal regions (e.g., auditory cortex) and multimodal areas (i.e., parahippocampus) in diametrically opposing directions which relate key physiological features (search for compensatory information and hard-wiring of regions) with behavioral symptoms (loudness and distress). This can explain the dynamics of other pathologies such as chronic pain and addiction, which are also hypothesized to be a maladaptive compensation to salient stimuli (De Ridder, Joos, & Vanneste, 2015; De Ridder, Manning, Leong, Ross, & Vanneste, 2016; De Ridder, Vanneste, Weisz, et al., 2014; De Ridder, Vanneste, & Freeman, 2014; De Ridder, Manning, Leong, Ross, Sutherland, et al., 2016). Further, the results of the current study can also be extrapolated to disorders characterized by patients stuck in a particular state such as depression, schizophrenia, Parkinson's disease, and can explain why some of these disorders may presently not have a cure.

4.1 | Limitations and strengths

The current study successfully investigates the temporal dynamics of functional connectivity in tinnitus but with some limitations. First, several studies show differential activation of cortical networks to the presence of hearing loss. However, the tinnitus population in current study is not controlled for hearing loss and hence future studies replicating the same methodology with a more controlled population would be worthwhile. Second, the study uses 19-channel EEG data and a low-resolution source localization technique to identify 84 Brodmann areas. The spatial resolution of the source localization of especially deeper structures such as the parahippocampus using 19 electrodes should be interpreted with care. Although the source localization using sLORETA has been shown to be accurate with 27 and 64 channel EEG, the low-density EEG used in this study still runs the risk of unreliability of localizing deeper structures in higher frequency bands. Thus, future studies could implement a null model to test the validity of the source localization using sLORETA and 19 channels. Further, the head model used for the localization and the location of the electrodes is based on the standard MNI template. In order to perform subject-level accurate source localization, future studies could use the individual MRI scans of the subjects and a digitizer to obtain the individual's scalp locations for the electrodes. The use of EEG-based source localization also limits the findings of the current technique only to cortical areas. However, the connections with mesolimbic structures have played a significant role may in modulating tinnitus loudness and distress. Thus, the replication of the current technique with high resolution

techniques will help confirming the results and investigating the dynamics of deeper subcortical structures.

The strength of the current study lies in the validation of the results using overlapping and nonoverlapping windows of different window lengths. The results of all three windows, although not exactly the same, closely follow the same trend, suggesting that our results are robust. Thus, the current study remains one of the first studies that investigates the temporal dynamics of functional connectivity and its relevance to domain-specific and domain-general aspects of a pathology. Furthermore, the effect of distress on the temporal dynamics of multimodal disorder general regions may be translated to other chronic pathologies that are known to be influenced by an affective component.

5 | CONCLUSION

The current study demonstrates maladaptive changes in temporal variability that could either reflect an increase in flexibility in temporal binding of brain regions, indicating rapid fluctuations of connectivity over time, or an increase in specificity of temporal binding, indicating more stable patterns of connectivity over time. These changes reflect disorder-specific and disorder-general physiological and behavioral manifestations of the pathology. Furthermore, the relationship between the behavioral and neural correlates depends on the amount of distress perceived by the patient, which suggests the presence of a critical point of transition between low and high distress below which the brain is resilient to changes and above which the brain is sensitive to change and possibly cascades into being hard-wired in that particular state. Changes in temporal binding witnessed on a network level and in unimodal and multimodal regions encode behavioral symptoms of tinnitus. These findings inform us about the changes in temporal dynamics of network connectivity in tinnitus and can potentially explain other pathologies.

ACKNOWLEDGEMENTS

We would like to thank Jeffrey Hullfish for his valuable comments on the manuscript.

CONFLICT OF INTEREST

The authors declare no competing financial interests.

RESEARCH INVOLVING HUMAN PARTICIPANTS

This study was approved by the local ethical committee (Antwerp University Hospital) and was in accordance with the Declaration of Helsinki. Collection of the data was under

approval of IRB UZA OGA85. All patients gave a written informed consent.

DATA ACCESSIBILITY

Data are present with the corresponding author and may be available on request.

AUTHORS' CONTRIBUTION

AM performed data analysis and wrote the manuscript. DDR: collected the data and wrote the manuscript. RI and CD: analyzed the data. SV collected the data, analyzed the data, and wrote the manuscript.

ORCID

Anusha Mohan  <http://orcid.org/0000-0003-1904-0603>

REFERENCES

- Adamchic, I., Langguth, B., Hauptmann, C., & Tass, P. A. (2012). Psychometric evaluation of visual analog scale for the assessment of chronic tinnitus. *American Journal of Audiology*, 21, 215–225.
- Arnsten, A. F. T., Paspalas, C. D., Gamo, N. J., Yang, Y., & Wang, M. (2010). Dynamic Network connectivity: A new form of neuroplasticity. *Trends in Cognitive Sciences*, 14, 365–375.
- Audiology. (2008). *Recommended procedure: Pure tone air and bone conduction threshold audiometry with and without masking and determination of uncomfortable loudness levels* (pp. 1–36). Retrieved from <http://www.thebsa.org.uk/wp-content/uploads/2017/02/Recommended-Procedure-Pure-Tone-Audiometry-Jan-2017-V2-1.pdf>
- Baguley, D. M., Humphriss, R. L., & Hodgson, C. A. (2000). Convergent validity of the tinnitus handicap inventory and the tinnitus questionnaire. *Journal of Laryngology and Otology*, 114, 840–843.
- Barttfeld, P., Petroni, A., Báez, S., Urquina, H., Sigman, M., Cetkovich, M., ... Castellanos, X. (2014). Functional connectivity and temporal variability of brain connections in adults with attention deficit/hyperactivity disorder and bipolar disorder. *Neuropsychobiology*, 69, 65–75.
- Bassett, D. S., Wymbs, N. F., Porter, M. A., Mucha, P. J., Carlson, J. M., & Grafton, S. T. (2011). Dynamic reconfiguration of human brain networks during learning. *Proceedings of the National Academy of Sciences*, 108, 7641–7646.
- Belli, S., Belli, H., Bahcebasi, T., Ozcetin, A., Alpay, E., & Ertem, U. (2007). Assessment of psychopathological aspects and psychiatric comorbidities in patients affected by tinnitus. *European Archives of Oto-Rhino-Laryngology*, 265, 279–285.
- Brett, M., Johnsrude, I. S., & Owen, A. M. (2002). The problem of functional localization in the human brain. *Nature Reviews Neuroscience*, 3, 243.
- Congedo, M. (2002). *EureKa! (Version 3.0) [Computer Software]*. Knoxville, TN: NovaTech EEG Inc. Freeware available at: www.NovaTechEEG
- Congedo, M., John, R. E., De Ridder, D., Prichep, L., & Isenhardt, R. (2010). On the “dependence” of “independent” group EEG sources;

- an EEG study on two large databases. *Brain Topography*, 23, 134–138.
- De Ridder, D., Congedo, M., & Vanneste, S. (2015). The neural correlates of subjectively perceived and passively matched loudness perception in auditory phantom perception. *Brain and Behavior*, 5, e00331.
- De Ridder, D., Elgoyhen, A. B., Romo, R., & Langguth, B. (2011). Phantom percepts: Tinnitus and pain as persisting aversive memory networks. *Proceedings of the National Academy of Sciences*, 108, 8075–8080.
- De Ridder, D., Joos, K., & Vanneste, S. (2015). Anterior cingulate implants for tinnitus: Report of 2 cases. *Journal of Neurosurgery*, 124, 893–901.
- De Ridder, D., Manning, P., Leong, S. L., Ross, S., Sutherland, W., Horwath, C., & Vanneste, S. (2016). The brain, obesity and addiction: An EEG neuroimaging study. *Scientific Reports*, 6, 34122.
- De Ridder, D., Manning, P., Leong, S. L., Ross, S., & Vanneste, S. (2016). Allostasis in health and food addiction. *Scientific Reports*, 6, 37126.
- De Ridder, D., & Vanneste, S. (2014). Targeting the parahippocampal area by auditory cortex stimulation in tinnitus. *Brain Stimulation*, 7, 709–717.
- De Ridder, D., Vanneste, S., & Congedo, M. (2011). The distressed brain: A group blind source separation analysis on tinnitus. *PLoS One*, 6, e24273.
- De Ridder, D., Vanneste, S., & Freeman, W. (2014). The Bayesian brain: Phantom percepts resolve sensory uncertainty. *Neuroscience and Biobehavioral Reviews*, 44, 4–15.
- De Ridder, D., Vanneste, S., Langguth, B., & Llinas, R. (2015). Thalamocortical Dysrhythmia: A theoretical update in tinnitus. *Frontiers in Neurology*, 6, 124.
- De Ridder, D., Vanneste, S., Weisz, N., Londero, A., Schlee, W., Elgoyhen, A. B., & Langguth, B. (2014). An integrative model of auditory phantom perception: Tinnitus as a unified percept of interacting separable subnetworks. *Neuroscience and Biobehavioral Reviews*, 44, 16–32.
- Deco, G., & Kringelbach, M. L. (2016). Metastability and coherence: Extending the communication through coherence hypothesis using a whole-brain computational perspective. *Trends in Neurosciences*, 39, 125–135.
- Deco, G., Tononi, G., Boly, M., & Kringelbach, M. L. (2015). Rethinking segregation and integration: Contributions of whole-brain modelling. *Nature Reviews Neuroscience*, 16, 430–439.
- Engel, A. K., & Singer, W. (2001). Temporal binding and the neural correlates of sensory awareness. *Trends in Cognitive Sciences*, 5, 16–25.
- Fecteau, J. H., & Munoz, D. P. (2006). Saliency, relevance, and firing: A priority map for target selection. *Trends in Cognitive Sciences*, 10, 382–390.
- Fox, M. D., Snyder, A. Z., Vincent, J. L., Corbetta, M., Van Essen, D. C., & Raichle, M. E. (2005). The human brain is intrinsically organized into dynamic, anticorrelated functional networks. *Proceedings of the National Academy of Sciences of the United States of America*, 102, 9673–9678.
- Fuchs, M., Kastner, J., Wagner, M., Hawes, S., & Ebersole, J. S. (2002). A standardized boundary element method volume conductor model. *Clinical Neurophysiology*, 113, 702–712.
- Goebel, G., & Hiller, W. (1994). The tinnitus questionnaire. A standard instrument for grading the degree of tinnitus. Results of a multicenter study with the tinnitus questionnaire. *HNO*, 42, 166–172.
- González-Roldán, A. M., Cifre, I., Sitges, C., & Montoya, P. (2016). Altered dynamic of EEG oscillations in fibromyalgia patients at rest. *Pain Medicine*, 17(6), 1058–1068.
- van den Heuvel, M. P., & Sporns, O. (2013). An anatomical substrate for integration among functional networks in human cortex. *The Journal of Neuroscience*, 33, 14489–14500.
- Hindriks, R., Adhikari, M. H., Murayama, Y., Ganzetti, M., Mantini, D., Logothetis, N. K., & Deco, G. (2016). Can sliding-window correlations reveal dynamic functional connectivity in resting-state fMRI? *NeuroImage*, 127, 242–256.
- Hutchison, R. M., Womelsdorf, T., Allen, E. A., Bandettini, P. A., Calhoun, V. D., Corbetta, M., ... Chang, C. (2013). Dynamic functional connectivity: Promise, issues, and interpretations. *NeuroImage*, 80, 360–378.
- Imperatori, C., Farina, B., Quintiliani, M. I., Onofri, A., Gattinara, P. C., Lepore, M., ... Della Marca, G. (2014). Aberrant EEG functional connectivity and EEG power spectra in resting state post-traumatic stress disorder: A sLORETA study. *Biological Psychology*, 102, 10–17.
- Jansen, E. J. M., Helleman, H. W., Dreschler, W. A., & de Laat, J. A. P. M. (2009). Noise induced hearing loss and other hearing complaints among musicians of symphony orchestras. *International Archives of Occupational and Environmental Health*, 82, 153–164.
- Jastreboff, P. J. (1990). Phantom auditory perception (tinnitus): Mechanisms of generation and perception. *Neuroscience Research*, 8, 221–254.
- Jurcak, V., Tsuzuki, D., & Dan, I. (2007). 10/20, 10/10, and 10/5 systems revisited: Their validity as relative head-surface-based positioning systems. *NeuroImage*, 34, 1600–1611.
- Kaiser, R. H., Whitfield-Gabrieli, S., Dillon, D. G., Goer, F., Beltzer, M., Minkel, J., ... Pizzagalli, D. A. (2015). Dynamic resting-state functional connectivity in major depression. *Neuropsychopharmacology*, 41, 1822–1830.
- Lancaster, J. L., Woldorff, M. G., Parsons, L. M., Liotti, M., Freitas, C. S., Rainey, L., ... Fox, P. T. (2000). Automated Talairach Atlas labels for functional brain mapping. *Human Brain Mapping*, 10, 120–131.
- Langers, D. R., de Kleine, E., & van Dijk, P. (2012). Tinnitus does not require macroscopic tonotopic map reorganization. *Frontiers in Systems Neuroscience*, 6, 2.
- von Leupoldt, A., Sommer, T., Kegat, S., Baumann, H. J., Klose, H., Dahme, B., & Büchel, C. (2009). Dyspnea and pain share emotion-related brain network. *NeuroImage*, 48, 200–206.
- van der Loo, E., Gais, S., Congedo, M., Vanneste, S., Plazier, M., Menovsky, T., ... De Ridder, D. (2009). Tinnitus intensity dependent gamma oscillations of the contralateral auditory cortex. *PLoS One*, 4, e7396.
- Maudoux, A., Lefebvre, P., Cabay, J.-E., Demertzi, A., Vanhaudenhuyse, A., Laureys, S., & Soddu, A. (2012). Auditory resting-state network connectivity in tinnitus: A functional MRI study. *PLoS One*, 7, e36222.
- Maudoux, A., Lefebvre, P., Cabay, J. E., Demertzi, A., Vanhaudenhuyse, A., Laureys, S., & Soddu, A. (2012). Connectivity graph analysis of the auditory resting state network in tinnitus. *Brain Research*, 1485, 10–21.
- Mazziotta, J., Toga, A., Evans, A., Fox, P., Lancaster, J., Zilles, K., ... Mazoyer, B. (2001). A probabilistic atlas and reference system for the human brain: International Consortium for Brain Mapping

- (ICBM). *Philosophical Transactions of the Royal Society of London. Series B*, 356, 1293–1322.
- Meeus, O., Blaivie, C., & Van de Heyning, P. (2007). Validation of the dutch and the french version of the tinnitus questionnaire. *B-ENT*, 3(Suppl. 7), 11–17.
- Meeus, O., De Ridder, D., & Van de Heyning, P. (2011). Administration of the combination clonazepam-deanxit as treatment for tinnitus. *Otology and Neurotology*, 32, 701–709.
- Meeus, O., Heyndrickx, K., Lambrechts, P., De Ridder, D., & Van de Heyning, P. (2009). Phase-shift treatment for tinnitus of cochlear origin. *European Archives of Oto-Rhino-Laryngology*, 267, 881–888.
- Mohan, A., Moreno, N., Song, J.-J., De Ridder, D., & Vanneste, S. (2017). Evidence for behaviorally segregated, spatiotemporally overlapping subnetworks in phantom sound perception. *Brain Connectivity*, 7, 197–210.
- Mohan, A., & Vanneste, S. (2017). Adaptive and maladaptive neural compensatory consequences of sensory deprivation—From a phantom percept perspective. *Progress in Neurobiology*, 153, 1–17.
- Pascual-Marqui, R. D. (2002). Standardized low-resolution brain electromagnetic tomography (sLORETA): Technical details. *Methods and Findings in Experimental and Clinical Pharmacology*, 24(Suppl. D), 5–12.
- Pascual-Marqui, R. D. (2007). Instantaneous and lagged measurements of linear and nonlinear dependence between groups of multivariate time series: Dfrequency decomposition. arXiv preprint arXiv:0711.1455.
- Pascual-Marqui, R. D., Lehmann, D., Koukkou, M., Kochi, K., Anderer, P., Saletu, B., ... Prichep, L. (2011). Assessing interactions in the brain with exact low-resolution electromagnetic tomography. *Philosophical Transactions of the Royal Society of London A: Mathematical, Physical and Engineering Sciences*, 369, 3768–3784.
- Plack, C. J., Barker, D., & Prendergast, G. (2014). Perceptual consequences of “Hidden” hearing loss. *Trends in Hearing*, 18, 2331216514550621.
- Plack, C. J., Prendergast, G., & Hall, D. A. (2015). Hidden hearing loss and tinnitus. *Journal of International Advanced Otology*, 11, 11.
- Stam, C. J. (2014). Modern network science of neurological disorders. *Nature Reviews Neuroscience*, 15, 683–695.
- Stark, M. (2012). The sandpile model: Optimal stress and hormesis. *Dose-Response*, 10, 66–74. dose-response. 11-010. Stark.
- Szymiec, E., Dabrowski, P., Banaszewski, J., & Szyfter, W. (2002). The problem of tinnitus in patients with presbycusis. *Otolaryngologia Polska*, 56, 357–360.
- Ueyama, T., Donishi, T., Ukai, S., Ikeda, Y., Hotomi, M., Yamanaka, N., ... Kaneoke, Y. (2013). Brain regions responsible for tinnitus distress and loudness: A resting-state fMRI study. *PLoS One*, 8, e67778.
- Vanneste, S., Congedo, M., & De Ridder, D. (2014). Pinpointing a highly specific pathological functional connection that turns phantom sound into distress. *Cerebral Cortex*, 24, 2268–2282.
- Vanneste, S., & De Ridder, D. (2015). Stress-related functional connectivity changes between auditory cortex and cingulate in tinnitus. *Brain Connectivity*, 5, 371–383.
- Vanneste, S., & De Ridder, D. (2016). Deafferentation-based pathophysiological differences in phantom sound: Tinnitus with and without hearing loss. *NeuroImage*, 129, 80–94.
- Vanneste, S., Plazier, M., der Loo, E. V., de Heyning, P. V., Congedo, M., & De Ridder, D. (2010). The neural correlates of tinnitus-related distress. *NeuroImage*, 52, 470–480.
- Vanneste, S., van de Heyning, P., & De Ridder, D. (2011). The neural network of phantom sound changes over time: A comparison between recent-onset and chronic tinnitus patients. *European Journal of Neuroscience*, 34, 718–731.
- Werff, S. J., Pannekoek, J. N., Stein, D. J., & Wee, N. J. (2013). Neuroimaging of resilience to stress: Current state of affairs. *Human Psychopharmacology: Clinical and Experimental*, 28, 529–532.
- Zeman, F., Koller, M., Figueiredo, R., Aazevedo, A., Rates, M., Coelho, C., ... Landgrebe, M. (2011). Tinnitus handicap inventory for evaluating treatment effects: Which changes are clinically relevant? *Otolaryngology-Head and Neck Surgery*, 145, 282–287.
- Zhang, J., Cheng, W., Liu, Z., Zhang, K., Lei, X., Yao, Y., ... Lu, G. (2016). Neural, electrophysiological and anatomical basis of brain-network variability and its characteristic changes in mental disorders. *Brain*, 139, 2307–2321.

SUPPORTING INFORMATION

Additional supporting information may be found online in the Supporting Information section at the end of the article.

How to cite this article: Mohan A, De Ridder D, Idiculla R, DSouza C, Vanneste S. Distress-dependent temporal variability of regions encoding domain-specific and domain-general behavioral manifestations of phantom percepts. *Eur J Neurosci*. 2018;00:1–22. <https://doi.org/10.1111/ejn.13988>